

---

**MPU: Towards Secure and Privacy-Preserving Knowledge Unlearning for Large Language Models**

---

Tiantong Wang<sup>1,2</sup> Xinyu Yan<sup>1,2</sup> Tiantong Wu<sup>1,2</sup> Yurong Hao<sup>1</sup>  
Yong Jiang<sup>3</sup> Fei Huang<sup>3</sup> Wei Yang Bryan Lim<sup>1</sup>

### Abstract

Machine unlearning for large language models often faces a privacy dilemma in which strict constraints prohibit sharing either the server’s parameters or the client’s forget set. To address this dual non-disclosure constraint, we propose **MPU**, an algorithm-agnostic privacy-preserving **M**ultiple **P**erturbed Copies **U**nlearning framework that primarily introduces two server-side modules: **Pre-Process** for randomized copy generation and **Post-Process** for update aggregation. In Pre-Process, the server distributes multiple perturbed and reparameterized model instances, allowing the client to execute unlearning locally on its private forget set without accessing the server’s exact original parameters. After local unlearning, the server performs Post-Process by inverting the reparameterization and aggregating updates with a harmonic denoising procedure to alleviate the impact of perturbation. Experiments with seven unlearning algorithms show that **MPU** achieves comparable unlearning performance to noise-free baselines, with most algorithms’ average degradation well below 1% under 10% noise, and can even outperform the noise-free baseline for some algorithms under 1% noise. Code is available at <https://github.com/Tristan-SHU/MPU>.

## 1. Introduction

As large language models (LLMs) continue to advance, their tendency to memorize and reproduce training data has raised serious concerns about privacy, safety, and intellectual property. These concerns motivate an urgent need for **machine unlearning** (Cao & Yang, 2015), whose goal

---

<sup>1</sup>College of Computing and Data Science, Nanyang Technological University, Singapore <sup>2</sup>Alibaba-NTU Global e-Sustainability CorpLab (ANGEL), Singapore <sup>3</sup>Tongyi Lab, Alibaba Group. Correspondence to: Wei Yang Bryan Lim <bryan.limwy@ntu.edu.sg>.

is to selectively remove undesired data, knowledge, or behaviors from a trained model while preserving its general utility for normal tasks. Unlearning is particularly challenging for modern LLMs, as full retraining is prohibitively expensive, and deletion requests may arrive continuously over the model’s lifecycle. As a result, a growing body of research has investigated approaches ranging from training-time strategies such as sharding or slicing (Bourtoule et al., 2021), post-hoc model editing and selective forgetting (Golatkar et al., 2020), influence-based approximations (Koh & Liang, 2017), and foundational formulations of deletion guarantees (Ginart et al., 2019).

However, many real-world deployments impose an additional constraint that is often overlooked: the data to be forgotten may belong confidentially to a client and must remain local, while the deployed model is proprietary to the server. This creates a central tension in **server-client unlearning**: the server requires an update that removes the effect of a client-local forget set, but (i) the client should not disclose raw data (or fine-grained sufficient statistics) to the server, and (ii) the server may prefer not to reveal its exact current model parameters to the client. Consequently, this setting calls for a restricted server-client unlearning framework that enables effective forgetting without direct data sharing, and without exposing the server’s exact parameters.

Existing unlearning approaches do not directly address this challenge. Training-time methods based on SISA-style sharding or slicing can reduce the deletion cost by retraining only affected subsets, but require maintaining specific training structures and retaining per-shard state to support subsequent retraining upon deletion requests (Bourtoule et al., 2021). Post-hoc techniques such as selective forgetting can lower the cost of removing particular classes or examples, but typically assume that the entity performing unlearning has direct access to the model and relevant data distributions (Golatkar et al., 2020). Influence-function-based approximations offer a principled lens on example influence. However, they can be computationally demanding for LLMs and often rely on second-order information that is difficult to obtain robustly at scale (Koh & Liang, 2017). In federated settings, the right to be forgotten has

been explored through reconstructing an unlearned model using server-side training histories (Liu et al., 2020) or by coordinating efficient retraining while keeping data local (Liu et al., 2022b). Recent work further highlights that federated unlearning methods can exhibit substantial trade-offs between effectiveness and efficiency across scenarios (Zhang et al., 2025). Overall, many existing solutions rely on substantial server-side state or centralized access to training records, exposing the server’s exact current model to clients.

In this paper, we propose MPU, a privacy-preserving Multiple Perturbed Copies Unlearning framework tailored to server–client deployments. Our key idea is to let the server publish perturbed model instances to clients, with the perturbation designed to be self-canceling during server-side aggregation. Specifically, at each communication round, instead of broadcasting the exact model parameters, the server releases  $m \geq 2$  copies that are (i) perturbed by structured noise and (ii) transformed by an invertible, data-independent, function-preserving reparameterization sampled from parameter symmetries. Starting from each published copy, the client runs a local unlearning routine on its private forget set and returns copy-wise updates. The server then inverts the reparameterizations and aggregates the returned updates using harmonic weights, which cancel the first-order error term introduced by noise. As a result, MPU yields a server-side update that matches the noise-free unlearning step, while keeping forget set local and obscuring the server’s exact model parameters by communicating only perturbed, symmetry-transformed copies. The key contributions are:

- **Dual Non-Disclosure Unlearning Framework.** We propose a server–client parameter-unlearning framework where the client keeps the forget set local (sharing neither raw data nor fine-grained sufficient statistics/distribution), while the server avoids disclosing its exact current parameters by communicating perturbed model copies. To our knowledge, this is the first solution to the dual non-disclosure setting without relying on auxiliary statistics, such as surrogate data.
- **Invertible and Function-Preserving Reparameterizations.** We generalize invertible, data-independent, function-preserving reparameterizations to modern Transformer architectures, including RoPE-style positional mechanisms, enabling symmetry-based reparameterizations for LLMs (e.g., Meta’s Llama family of models).
- **Theoretical Guarantees for First-Order Noise Cancellation.** We provide theoretical guarantees that, under our structured noise injection and harmonic aggregation, the first-order error induced by noise is eliminated after aggregation, resulting in a server update that is consistent with the noise-free unlearning step.

- **Empirical Evaluation.** We empirically evaluate MPU on representative LLM unlearning tasks, demonstrating effective forgetting while maintaining model utility under the server-client deployment constraints.

## 2. Related Works

### 2.1. LLM Unlearning

LLMs acquire vast amounts of knowledge during pre-training, which may include sensitive or otherwise undesired information (Qiu et al., 2025). Machine unlearning aims to enable models to “forget” specific pieces of knowledge while maintaining performance on remaining data. Recent work has therefore focused on selective unlearning, i.e., suppressing undesired outputs for a designated forget set. Text-based strategies include Gradient Ascent fine-tuning that maximizes cross-entropy loss on forget samples (Jang et al., 2023; Yao et al., 2024), preference-inspired objectives (e.g., NPO and SimNPO) that constrain updates with a reference model and length-normalized rewards (Zhang et al., 2024; Fan et al., 2024), and substitute-response training that learns safe alternative answers to forget queries (Maini et al., 2024; Mekala et al., 2025).

Beyond text-level objectives, distribution-based approaches drive the model’s output distribution toward a target distribution aligned with unlearning goals (Liu et al., 2025; Wang et al., 2025). Meanwhile, activation-based methods intervene on internal representations rather than only on outputs, for example, by perturbing hidden states for harmful inputs toward random or refusal-like directions (Shen et al., 2025). Rather than weighting multiple losses, recent works such as NGDiff and MoLLM (Jin et al., 2025; Pan et al., 2025) formulate the combination as a multi-task problem, normalizing gradients and computing common descent directions to better trade off forgetting target knowledge against retaining overall utility. However, many existing LLM unlearning algorithms are studied in settings where the unlearning party can access the model parameters and optimize using the forget set. In this work, we focus on a more constrained server-client deployment in which the forget set remains client-local, and the server does not expose its parameters during the unlearning process.

### 2.2. Direct Model Merging

Our framework aggregates multi-copy updates computed from multiple models, which relates to direct model merging and the empirical linearity of parameter updates in the fine-tuning paradigm. In this paradigm, models adapted to different tasks from a shared pretrained checkpoint often exhibit cross-task linearity, whereby their weights and feature spaces can be combined through linear interpolation, enabling direct model merging without additional retraining

and substantially reducing computational overhead (Zhou et al., 2024b). A widely used strategy is weight averaging, where parameters of similarly initialized fine-tuned models are averaged. Model Soups (Wortsman et al., 2022) further demonstrated that such averaging can improve accuracy and out-of-distribution robustness compared to individual models. Alternatively, task arithmetic operates on task vectors to compose or edit specific model capabilities.

More recently, Zhou et al. (2024a) extended task arithmetic to LLMs, formulating it as an optimization problem that exploits local linearity and near-orthogonality of task updates. While these works primarily aim to compose task-specific capabilities, they are not designed for unlearning under server-client confidentiality constraints. In our setting, we exploit the local linearity of copy-wise updates to enable aggregation across copies with error cancellation.

### 3. Proposed Method: MPU

#### 3.1. Overview

We consider a server-client unlearning framework operating over  $R$  communication rounds. Each round consists of three sequential stages. First, the server generates and distributes  $m$  perturbed copies of the current global model to the client. Second, the client performs local unlearning on these perturbed models using its private dataset. Lastly, the server collects the resulting local unlearning updates and aggregates them via a harmonic denoising mechanism, producing the updated global model for the next round.

#### 3.2. Pre-Process: Perturbed Copies Generation

In each round, the server perturbs the current model before transmitting it to the client. The generation of perturbed copies consists of two components: (i) structured noise injection and (ii) an invertible, function-preserving reparameterization. Noise injection mitigates privacy leakage risks during inference. Meanwhile, the reparameterization obscures the original parameter space, preventing the client from reconstructing the original parameters even when multiple perturbed copies are accessed.

##### 3.2.1. NOISE GENERATION

Noise injection is a common and effective defense against inference attacks. In MPU, noise is generated independently per block  $\ell$  with scale  $\sigma_\ell$ . We set  $\sigma_\ell$  based on a reference task vector  $v_\ell$ , defined as the difference between the current model parameters and a public reference model parameter. Here, the public reference model refers to a released pre-trained model before fine-tuning. This design is motivated by the fact that the task vector captures the parameter update induced by fine-tuning, which possibly may encode sensitive information about the underlying private data.

---

#### Algorithm 1 MPU

---

**Require:**  $\theta_0, R, m \geq 2, \{\sigma_\ell\}, \{\alpha_k > 0\}_{k=1}^m, \eta_{\text{srv}}, \{s_r\}_{r=1}^R, \{t_r\}_{r=1}^R$

- 1: **for**  $r = 1$  **to**  $R$  **do**
- 2:   Base Noise (Sec. 3.2.1): Generate  $\{\epsilon_{k,\ell}^{0,(r)}\}$  from seed  $s_r$  using Eq. (2) (for all  $k \in [m]$  and blocks  $\ell$ )
- 3:   Copy Scaling (Sec. 3.2.1): For each  $k$ , scaling the noise  $\epsilon_{k,\ell}^{(r)} \leftarrow \alpha_k \epsilon_{k,\ell}^{0,(r)}$  and stack  $\epsilon_k^{(r)} := \text{stack}_\ell(\epsilon_{k,\ell}^{(r)})$
- 4:   Initialize Accumulators:  $S_0 \leftarrow 0; S_1 \leftarrow \mathbf{0} \in \mathbb{R}^d$
- 5:   **for**  $k = 1$  **to**  $m$  **do**
- 6:     Server Sample Reparameterization (Sec. 3.2.2):  $T_{k,r} \leftarrow \text{SAMPLEREPARAM}(t_r, k)$
- 7:     Publish Copy:  $\theta_{\text{pub}}^{(k,r)} \leftarrow T_{k,r}(\theta_{r-1} + \epsilon_k^{(r)})$
- 8:     Client Returns:  $\Delta^{(k,r)} \leftarrow \text{UNLEARN}(\theta_{\text{pub}}^{(k,r)}, \mathcal{D}_f)$
- 9:     Server Invert Reparameterization:  $\bar{\Delta}^{(k,r)} \leftarrow T_{k,r}^{-1}(\Delta^{(k,r)})$
- 10:    Accumulate Harmonic-Weighted Updates:  $S_0 \leftarrow S_0 + \alpha_k^{-1}; S_1 \leftarrow S_1 + \alpha_k^{-1} \bar{\Delta}^{(k,r)}$
- 11:    **end for**
- 12:    Harmonic Aggregation (Sec. 3.4):  $\bar{\Delta}^{(r)} \leftarrow S_1/S_0$
- 13:    Server Update:  $\theta_r \leftarrow \theta_{r-1} + \eta_{\text{srv}} \bar{\Delta}^{(r)}$
- 14: **end for**
- 15: **Return**  $\theta_R$

---

$$\sigma_\ell = \kappa \cdot \text{RMS}(v_\ell), \quad \text{RMS}(v_\ell) := \sqrt{\frac{1}{d_\ell} \sum_{t=1}^{d_\ell} v_\ell(t)^2}, \quad (1)$$

where  $\kappa > 0$  is a tunable noise-level hyperparameter.

For each round  $r$  and block  $\ell$ , the server draws i.i.d. Gaussian vectors  $z_{k,\ell}^{(r)} \sim \mathcal{N}(0, \sigma_\ell^2 I_{d_\ell})$  for  $k \in [m]$  from seeds  $s_r$  and  $l$ , subtracts their mean, and rescales the resulting vectors so that each perturbed copy maintains the prescribed marginal variance. The resulting base noise vectors satisfy a block-wise zero-sum constraint:

$$\epsilon_{k,\ell}^{0,(r)} = \sqrt{\frac{m}{m-1}} \left( z_{k,\ell}^{(r)} - \bar{z}_\ell^{(r)} \right) \Rightarrow \sum_{k=1}^m \epsilon_{k,\ell}^{0,(r)} \equiv 0, \quad (2)$$

where  $\bar{z}_\ell^{(r)} = \frac{1}{m} \sum_{k=1}^m z_{k,\ell}^{(r)}$ . Intuitively, the zero-sum structure forces the  $m$  copy noises to lie in an  $(m-1)$ -dimensional subspace, which is the key algebraic property enabling cancellation after aggregation.

We then apply a per-copy positive scaling  $\alpha_k > 0$ :

$$\epsilon_{k,\ell}^{(r)} = \alpha_k \epsilon_{k,\ell}^{0,(r)}, \quad \epsilon_k^{(r)} := \text{stack}_\ell(\epsilon_{k,\ell}^{(r)}) \in \mathbb{R}^d. \quad (3)$$

The  $\alpha_k$ 's introduce heterogeneous noise magnitudes across copies, work as a secondary protection, avoiding parameter reconstruction even if reparameterization information is leaked. Finally, we add the noise  $\epsilon_k^{(r)}$  to the original model parameters to obtain  $m$  first-stage perturbed models prior to reparameterization.

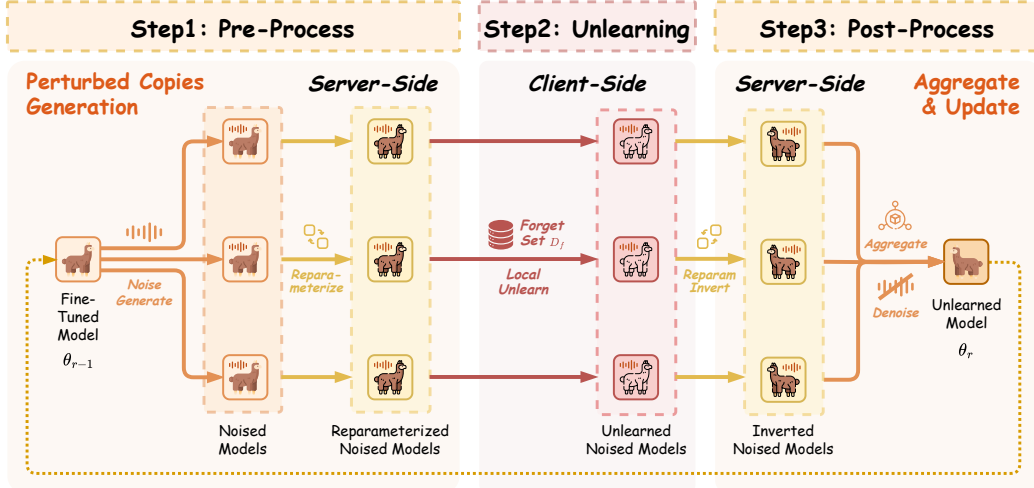


Figure 1. Overview of the proposed **MPU** framework across communication rounds. The server generates perturbed, reparameterized model copies from  $\theta_{r-1}$ , clients unlearn on  $D_f$ , and the server inverts the reparameterization and aggregates updates to obtain  $\theta_r$ .

**Connection to Differential Privacy** In standard noise-injection privacy mechanisms such as Differential Privacy (DP) (Mironov, 2017), one typically specifies a privacy budget first (e.g.,  $(\epsilon, \delta)$ ), and then calibrates the noise level according to a chosen DP algorithm and its accounting method. In practice, the resulting noise scale can vary across different DP mechanisms as well as with hyperparameters used by the algorithm. For simplicity and consistency, we therefore use a fixed noise level directly in **MPU**.

### 3.2.2. REPARAMETERIZATION

To prevent client-side reconstruction of the original model from multiple copies, the server applies a reparameterization to each block prior to releasing the perturbed models. We derive functionally invariant reparameterization on Transformer model architectures (Vaswani et al., 2017), extending previous work on neural network functional invariance (Kůrková & Kainen, 1994).

Let  $\Theta$  denote the parameter tuple of an attention or feed-forward network (FFN) block, and let  $f_\Theta : \mathbb{R}^{d_{\text{model}}} \rightarrow \mathbb{R}^{d_{\text{model}}}$  denote the forward function induced by  $\Theta$ . We consider a family of *reparameterizations* acting on the parameter space, defined as invertible mappings  $T : \Theta \mapsto T(\Theta)$  equipped with explicit inverses  $T^{-1}$ .

For each copy  $k$  and round  $r$ , the server samples a distinct data-independent reparameterization

$$T_{k,r} \leftarrow \text{SAMPLEREPARAM}(t_r, k), \quad (4)$$

where  $T_{k,r}$  is dependent on solely seed  $t_r$  and  $k$ , which is *function-preserving*, i.e.,

$$f_{T_{k,r}(\Theta)}(x) = f_\Theta(x), \quad \forall x \in \mathbb{R}^{d_{\text{model}}}. \quad (5)$$

Equivalently, letting  $\mathcal{G}$  denote the set of all such invertible function-preserving maps,  $\mathcal{G}$  forms a *parameter-symmetry*

*group* under composition. Each  $T_{k,r} \in \mathcal{G}$  acts on  $\Theta$  while leaving the realized function invariant.

**Feed-Forward Network Reparameterization** For concreteness, we illustrate an example of reparameterization for an FFN block. Consider an FFN block with parameter tuple:

$$\Theta_{\text{FFN}} = (W_1, b_1, W_2, b_2), \quad (6)$$

where  $W_1 \in \mathbb{R}^{d_{\text{ff}} \times d_{\text{model}}}$ ,  $b_1 \in \mathbb{R}^{d_{\text{ff}}}$ ,  $W_2 \in \mathbb{R}^{d_{\text{model}} \times d_{\text{ff}}}$ , and  $b_2 \in \mathbb{R}^{d_{\text{model}}}$ .

The FFN implements the mapping

$$f_\Theta(x) = W_2 \sigma(W_1 x + b_1) + b_2, \quad (7)$$

for  $x \in \mathbb{R}^{d_{\text{model}}}$ , where  $\sigma$  denotes an element-wise activation function.

Let  $G_{\text{FFN}} := S_{d_{\text{ff}}}$  denote the symmetric group acting on the  $d_{\text{ff}}$  hidden channels, represented by permutation matrices  $P_\pi \in \mathbb{R}^{d_{\text{ff}} \times d_{\text{ff}}}$  for  $\pi \in S_{d_{\text{ff}}}$  (with  $P_\pi^{-1} = P_\pi^\top$ ). We define a group action  $\varphi$  as

$$\varphi(\pi, \Theta_{\text{FFN}}) = (P_\pi W_1, P_\pi b_1, W_2 P_\pi^\top, b_2). \quad (8)$$

Since  $\sigma$  is applied element-wise, it is permutation-equivariant:

$$\sigma(P_\pi z) = P_\pi \sigma(z), \quad \forall z \in \mathbb{R}^{d_{\text{ff}}}. \quad (9)$$

Consequently, for any  $\pi \in S_{d_{\text{ff}}}$  and any input  $x$ , choosing  $T_{k,r}(\cdot) = \varphi(\pi, \cdot)$  yields

$$\begin{aligned} f_{T_{k,r}(\Theta_{\text{FFN}})}(x) &= W_2 P_\pi^\top \sigma(P_\pi (W_1 x + b_1)) + b_2 \\ &= W_2 P_\pi^\top P_\pi \sigma(W_1 x + b_1) + b_2 \\ &= W_2 \sigma(W_1 x + b_1) + b_2 \\ &= f_{\Theta_{\text{FFN}}}(x), \end{aligned} \quad (10)$$

which demonstrates that permuting the FFN hidden channels yields a *functionally equivalent* reparameterization.

**Attention Reparameterization** More generally, Attention blocks admit a rich parameter-symmetry group that includes (i) discrete permutation symmetries (e.g., hidden-channel permutations within FFN-style submodules) and (ii) continuous attention symmetries corresponding to invertible basis changes within attention head subspaces (e.g., per-head orthogonal transformations) that leave the attention computation invariant. We provide detailed reparameterization constructions and invariance proofs for the full Transformer architecture in Appendix A.3.

For RoPE-based models such as Llama series models, we restrict attention transformations to those that commute with the RoPE operators, ensuring that the reparameterization preserves functional equivalence for both RoPE and non-RoPE network structures. Concrete forward and inverse formulas, along with the RoPE-commuting specialization, are presented in Appendix A.3.2.

**Optimization Trajectory Invariance** The reparameterization is not only function-preserving, but also induces an invariant optimization (learning) trajectory. Specifically, suppose  $\mathcal{A}$  is a deterministic learning algorithm (e.g., stochastic gradient descent with fixed mini-batch ordering). Then the learning dynamics satisfy Eq. 11:

$$\mathcal{A}(\theta) = T^{-1}(\mathcal{A}(T(\theta))), \quad (11)$$

indicating that optimization commutes with the reparameterization, so the local unlearning process will not be affected by reparameterization. Meanwhile, we also provide the detailed analysis of trajectory invariance in Appendix A.4.

### 3.3. Client-Side Local Unlearning

Upon receiving the reparameterized model parameters, the client performs local unlearning using its private data, employing standard unlearning algorithms such as GradAscent, NPO, and DPO. Notably, MPU is algorithm-agnostic and can be integrated with any parameter-based unlearning methods.

### 3.4. Post-Process: Update Aggregation

After the client returns the local unlearning update  $\Delta^{(k,r)}$ , the server maps it back to the original parameter coordinates using the explicit inverse reparameterization:

$$\widehat{\Delta}^{(k,r)} \leftarrow T_{k,r}^{-1}(\Delta^{(k,r)}), \quad (12)$$

so that all copy-wise updates are expressed in a common parameterization prior to aggregation. Note that  $T_{k,r}^{-1}$  is efficiently computable due to the property  $P_\pi^{-1} = P_\pi^\top$  for permutation-based reparameterizations (cf. Equation (8)).

After inversion, the server aggregates the  $m$  returned updates

using harmonic aggregation to cancel the first-order noise:

$$\bar{\Delta}^{(r)} = \frac{\sum_{k=1}^m \alpha_k^{-1} \widehat{\Delta}^{(k,r)}}{\sum_{k=1}^m \alpha_k^{-1}}. \quad (13)$$

Here, we briefly explain why the aggregation cancels the first-order noise. Let  $\Delta^*(\theta)$  denote the ideal (noise-free) unlearning displacement, and let  $J$  be the Jacobian of  $\Delta^*$  evaluated at  $\theta_{r-1}$ . Under a local linearization assumption, the inverted update first-order approximately satisfies

$$\widehat{\Delta}^{(k,r)} \approx \Delta^*(\theta_{r-1}) + J \epsilon_k^{(r)} = \Delta^*(\theta_{r-1}) + J \alpha_k \epsilon_k^{0,(r)}, \quad (14)$$

where  $\epsilon_k^{0,(r)}$  is the stacked noise before scaling. Substituting this expression into the harmonic average, the injected term becomes

$$\frac{\sum_{k=1}^m \alpha_k^{-1} J \alpha_k \epsilon_k^{0,(r)}}{\sum_{k=1}^m \alpha_k^{-1}} = \frac{J \sum_{k=1}^m \epsilon_k^{0,(r)}}{\sum_{k=1}^m \alpha_k^{-1}} = 0, \quad (15)$$

where the last equality follows from the block-wise zero-sum property in Eq. (2). Therefore, the aggregation eliminates the correlated first-order noise error, while requiring only the scalar coefficients  $\{\alpha_k\}$  rather than storing the full noise parameters. A more detailed error analysis for higher orders is provided in Appendix A.2.

At the end of each round, the server applies the aggregated update with step size  $\eta_{\text{srv}}$ :

$$\theta_r \leftarrow \theta_{r-1} + \eta_{\text{srv}} \bar{\Delta}^{(r)}. \quad (16)$$

### 3.5. Memory-Efficiency Implementation

Although Algorithm 1 conceptually adopts  $m$  published copies per round, the server and client do not need to store all  $m$  perturbed models (nor the  $m$  returned updates) in memory. This observation follows from the fact that the harmonic aggregation coefficient depends solely on  $\alpha_k$ 's. Consequently, the sufficient statistics for each round reduce to the two accumulators:

$$S_0 = \sum_{k=1}^m \alpha_k^{-1}, \quad S_1 = \sum_{k=1}^m \alpha_k^{-1} \widehat{\Delta}^{(k,r)} \in \mathbb{R}^d, \quad (17)$$

after which the update is given by  $\bar{\Delta}^{(r)} = S_1/S_0$ .

Concretely, the server can implement each round in a streaming manner. For  $k = 1, \dots, m$ , the server publishes only a single perturbed copy  $\theta_{\text{pub}}^{(k,r)} = T_{k,r}(\theta_{r-1} + \epsilon_k^{(r)})$ , receives the corresponding client update  $\Delta^{(k,r)}$ , inverts it as  $\widehat{\Delta}^{(k,r)} = T_{k,r}^{-1}(\Delta^{(k,r)})$ , and updates the accumulators:

$$S_0 \leftarrow S_0 + \alpha_k^{-1}, \quad S_1 \leftarrow S_1 + \alpha_k^{-1} \widehat{\Delta}^{(k,r)}. \quad (18)$$

At no point does the server need to store all  $m$  models or all  $m$  updates. The peak server-side memory footprint (beyond

Table 1. Performance comparison of different unlearning algorithms using the **Llama-3.2-1B** and **Qwen2.5-1.5B** models on the TOFU benchmark (Split99). Results are reported under three settings: *Clean*, a noise-free baseline; *Noised*, a single-copy noise baseline with the same noise magnitude but without denoising; and **MPU**, using  $m=2$  copies with noise level  $\kappa=0.01$ . Higher values indicate better performance for Forget Quality, Forget Truth Ratio, and Model Utility, while values of PrivLeak closer to 0 are preferred.

Unlearning Algorithms	Forget Quality $\uparrow$			Forget Truth Ratio $\uparrow$			Model Utility $\uparrow$			PrivLeak		
	CLEAN	NOISED	MPU	CLEAN	NOISED	MPU	CLEAN	NOISED	MPU	CLEAN	NOISED	MPU
<b>Llama-3.2-1B-Instruct</b>												
GRADASCENT [ACL 2023]	6.58e-5	2.81e-8	<b>5.41e-2</b>	0.355	0.246	<b>0.468</b>	0.000	0.000	<b>2.31e-4</b>	65.8	<b>58.9</b>	69.6
GRADDIFF [PMLR 2022]	0.405	0.266	<b>0.405</b>	0.535	0.533	<b>0.547</b>	0.461	0.461	<b>0.464</b>	77.1	<b>73.3</b>	77.2
DPO [NEURIPS 2023]	0.165	0.165	<b>0.266</b>	0.637	0.620	<b>0.641</b>	0.591	0.591	<b>0.595</b>	-25.5	<b>-19.8</b>	-28.9
NPO [COLM 2024]	0.919	0.766	<b>0.919</b>	0.624	<b>0.640</b>	0.628	0.599	<b>0.600</b>	0.597	30.6	32.9	<b>28.2</b>
SIMNPO [NEURIPS 2025]	5.41e-2	5.41e-2	<b>9.71e-2</b>	<b>0.526</b>	0.522	0.525	0.598	0.592	<b>0.598</b>	<b>-68.4</b>	-70.2	-71.8
UNDIAL [NAACL 2025]	<b>1.43e-2</b>	<b>1.43e-2</b>	<b>1.43e-2</b>	<b>0.530</b>	0.527	0.529	0.613	0.614	<b>0.615</b>	<b>-76.4</b>	-77.4	-78.0
SATIMP [ICML2025]	3.02e-3	6.76e-3	<b>6.76e-3</b>	0.474	0.470	<b>0.476</b>	0.600	0.597	<b>0.601</b>	-98.9	-99.1	<b>-98.9</b>
<b>Qwen2.5-1.5B-Instruct</b>												
GRADASCENT [ACL 2023]	1.43e-2	5.41e-2	<b>0.990</b>	0.516	0.536	<b>0.740</b>	9.75e-4	6.76e-4	<b>0.346</b>	<b>13.7</b>	62.1	-21.7
GRADDIFF [PMLR 2022]	6.58e-5	6.61e-6	<b>0.990</b>	0.622	0.586	<b>0.740</b>	0.297	0.322	<b>0.346</b>	80.9	76.7	<b>-21.6</b>
DPO [NEURIPS 2023]	0.266	0.405	<b>0.990</b>	<b>0.757</b>	0.750	0.738	0.305	0.335	<b>0.347</b>	86.0	87.5	<b>-21.7</b>
NPO [COLM 2024]	1.43e-2	2.86e-2	<b>0.919</b>	0.708	0.709	<b>0.739</b>	0.305	0.318	<b>0.346</b>	89.4	90.2	<b>-21.9</b>
SIMNPO [NEURIPS 2025]	0.990	0.990	<b>0.990</b>	0.738	<b>0.742</b>	0.738	0.349	<b>0.350</b>	0.347	-18.7	<b>-17.4</b>	-22.0
UNDIAL [NAACL 2025]	<b>1.000</b>	1.000	0.990	<b>0.769</b>	0.767	0.740	0.338	0.333	<b>0.346</b>	<b>12.3</b>	14.1	-21.8
SATIMP [ICML2025]	0.919	0.919	<b>0.990</b>	0.738	0.740	<b>0.740</b>	<b>0.349</b>	0.348	0.346	-21.8	<b>-20.5</b>	-21.5

the base parameters  $\theta_{r-1}$ ) is therefore dominated by a single  $d$ -dimensional accumulator  $S_1$  and the currently processed copy, yielding an  $O(d)$  memory requirement rather than  $O(md)$ . The same streaming procedure applies on the client side, where the client processes one published copy at a time, avoiding the need to store  $m$  models simultaneously.

## 4. Experiments

### 4.1. Experimental Setup

To evaluate the effectiveness of the proposed **MPU** framework when coupled with diverse unlearning algorithms, we design and conduct a comprehensive set of experiments.

#### 4.1.1. MODELS AND BENCHMARK

We conduct experiments using four representative base models: **Llama-3.2-1B-Instruct**, **Llama-3.2-3B-Instruct** (Grattafiori et al., 2024), **Qwen2.5-1.5B-Instruct** and **Qwen2.5-3B-Instruct** (Qwen et al., 2024). Both models are evaluated on the widely adopted **TOFU** benchmark (Maini et al., 2024), following established experimental setups in prior works (Wang et al., 2024; Dorna et al., 2025). The TOFU dataset consists of four subsets: **Forget** set, **Retain** set, **Real Authors (RA)**, and **World Facts (WF)**. We evaluate all methods under the standard **Split99** setting, where 1% of the data are designated for forgetting, and the remaining 99% are retained via a stratified partition.

#### 4.1.2. METRICS

We evaluate unlearning algorithms along three complementary dimensions: **Memorization**, **Privacy**, and **Util-**

**ity**. Following the TOFU benchmark settings, we report Forget Quality (FQ), Model Utility (MU), Forget Truth Ratio (FTR), and Privacy Leakage (PrivLeak), all computed according to the official benchmark definitions. We also provide a reference to the metrics details in Appendix B.2.

To assess how effectively **MPU** enables targeted forgetting while preserving general knowledge, we focus on two core metrics: **ROUGE** and **Probability**. These metrics characterize forgetting behavior from complementary perspectives. Specifically, Forget ROUGE measures the ROUGE-L (Lin, 2004) recall between generated responses and ground-truth answers on the Forget Set, indicating whether the model continues to reproduce forgotten content at the textual level. Forget Probability captures the conditional probability assigned to correct answers, providing a finer-grained signal that reflects changes in the model’s output distribution beyond surface-level text similarity.

#### 4.1.3. UNLEARNING ALGORITHMS

To contextualize our results, we benchmark **MPU** against representative unlearning objectives spanning distinct algorithmic paradigms, organized by the primary mechanism used to suppress information associated with the forget set:

- **Loss-Reversal, First-Order Unlearning:** Methods, including **GradAscent** (Jang et al., 2023) and **GradDiff** (Liu et al., 2022a), reverse the training signal on the forget set by maximizing the standard loss, optionally regularized by an explicit retain term.
- **Preference-Style, Bounded Objectives:** We further evaluate preference-style formulations: **DPO** (Rafailov

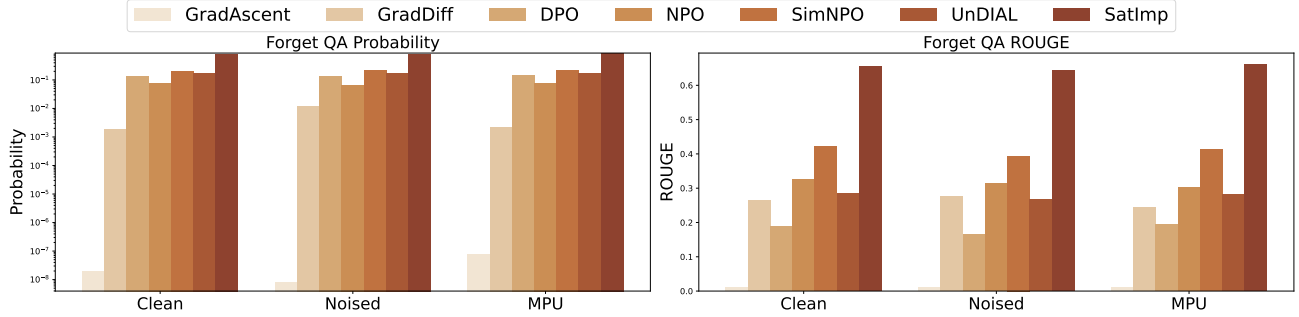


Figure 2. Performance comparison of different unlearning algorithms using the **Llama-3.2-1B** model. Results are reported under three settings: **Clean**, a noise-free baseline; **Noised**, a single-copy noise baseline with the same noise magnitude but without denoising; and **MPU**, using  $m=2$  copies with noise level  $\kappa=0.01$ . Higher values indicate better performance for Forget QA Probability and ROUGE.

et al., 2023), **NPO** (Zhang et al., 2024), and **SimNPO** (Fan et al., 2024), which replace unbounded loss maximization with bounded log-sigmoid objectives and improve optimization stability in practice.

- **Distribution Shaping via Self-Distillation:** Rather than directly increasing the forget loss, this paradigm distills the model toward an alternative target distribution that down-weights memorized content. **UnDIAL** (Dong et al., 2025) serves as the representative.
- **Loss Reweighting for Targeted Forgetting:** We consider adaptive reweighting strategies that modulate token- or sample-level contributions during optimization without explicit preference modeling. This family is instantiated by **SatImp** (Yang et al., 2025).

#### 4.1.4. BASELINES

Since **MPU** is designed to perform denoising after noisy perturbation, we compare it against two baselines. (i) **CLEAN**: a noise-free, centralized single-copy unlearning setting, corresponding to the standard unlearning framework with full access to the data and model and without any noise injection. The **CLEAN** baseline serves as an approximate upper bound on unlearning performance. (ii) **NOISED** (Appx. A.5): a single-copy baseline in which noise is directly injected before model publication, and the server adopts the client’s returned update without any denoising. **NOISED** provides a lower-bound reference for isolating the effect of denoising.

## 4.2. Experimental Results

### 4.2.1. MAIN RESULTS

**Privacy** Privacy measures whether sensitive data in the forget set can still be retrieved from the model. As shown in Table 1, we find that **MPU** under a low noise level consistently outperforms single-copy noised/noise-free unlearning in Forget Quality (FQ). Specifically, for unlearning algorithms with high FQ (**GradDiff**, **NPO**), **MPU** matches the

FQ of noise-free unlearning while substantially outperforming single-copy noisy unlearning, with 0.405 vs. 0.266 for **GradDiff**, and 0.919 vs. 0.766 for **NPO**. For other low-FQ unlearning algorithms (**GradAscent**, **SimNPO**, and **DPO**), we observe that the single-copy noisy and noise-free frameworks yield similar FQ scores, whereas **MPU** improves over both baselines significantly: 0.054 vs. near zero for **GradAscent**, 0.097 vs. 0.054 for **SimNPO**, and 0.266 vs. 0.165 for **DPO**. The increase in FQ relative to noise-free unlearning can be attributed to the multi-copy stability effect. For more details, please refer to Appendix A.6.

For Forget Truth Ratio (FTR) and PrivLeak (PL), we do not observe significant differences across the compared settings. This suggests that, under these two privacy-related metrics, all unlearning algorithms except **GradAscent** exhibit stable behavior. Comparing across unlearning algorithms, **NPO** performs best overall, achieving the highest average FQ and FTR together with the smallest absolute value of PL. Conversely, **GradAscent** exhibits almost zero FQ and MU under both the noise-free and single-copy noisy unlearning frameworks, indicating a complete breakdown of the model.

**Utility** Utility measures model performance on general tasks, reflecting whether general capability is preserved after unlearning. Table 1 shows that single-copy noise, noise-free unlearning, and **MPU** achieve very similar MU under each unlearning algorithm, with variations below 0.01. This indicates that utility preservation is not particularly sensitive to noise injection in our setup.

**Memorization** Memorization measures the extent to which the model retains information from the training data. From Figure 2, the Forget QA Probability of **MPU** is higher than the single-copy noise-free/no-denoise frameworks, except for the **SimNPO** algorithm (while only 0.002 lower compared with the noise-free one). The Forget QA ROUGE results show that **MPU** and the noise-free framework attain similar scores, while both outperform the no-denoise frame-

Table 2. Performance comparison of different unlearning algorithms using the **Llama-3.2-1B** model under **MPU** on the TOFU benchmark (Split99), with varying numbers of perturbed copies  $m \in \{2, 3, 4\}$  and noise level  $\kappa=0.01$ .

Unlearning Algorithms	Forget Quality $\uparrow$			Forget Truth Ratio $\uparrow$		
	$m=2$	$m=3$	$m=4$	$m=2$	$m=3$	$m=4$
GRADASCENT	5.41e-2	<b>0.165</b>	2.16e-5	0.468	<b>0.500</b>	0.334
GRADDIFF	0.405	0.405	<b>0.579</b>	0.547	0.555	<b>0.570</b>
DPO	0.266	<b>0.579</b>	0.165	<b>0.641</b>	0.631	0.615
NPO	<b>0.919</b>	0.766	0.766	<b>0.628</b>	0.623	0.620
SIMNPO	<b>9.71e-2</b>	5.41e-2	5.41e-2	<b>0.525</b>	0.518	0.519
UNDIAL	<b>1.43e-2</b>	1.43e-2	6.76e-3	<b>0.529</b>	0.528	0.528
SATIMP	6.76e-3	<b>1.43e-2</b>	3.02e-3	<b>0.476</b>	0.473	0.471

work. Moreover, **MPU** achieves the best ROUGE for the unlearning algorithms like **GradAscent**, **DPO**, and **SatImp**, whereas the noise-free framework yields the best ROUGE for **NPO**, **SimNPO**, and **SaImp**. Overall, these memorization results suggest that direct noise injection can introduce undesirable memorization artifacts, while **MPU** mitigates this effect via harmonic denoising aggregation.

#### 4.2.2. QWEN RESULT

As shown in Table 1, **MPU** consistently outperforms all baseline methods across the four evaluation metrics, demonstrating strong stability under different unlearning settings. Across various unlearning algorithms, **MPU** exhibits only minor performance variations and achieves superior results compared to the CLEAN and NOISED baselines in most cases. In particular, **MPU** maintains highly stable Forget Quality scores, all exceeding 0.9. In contrast, GradAscent, GradDiff, and NPO yield FQ values below 0.01, indicating ineffective unlearning. Moreover, **MPU** achieves higher Model Utility than the baseline methods in five out of seven unlearning algorithms, suggesting that it better preserves model performance while avoiding excessive unlearning.

#### 4.2.3. HYPERPARAMETER ANALYSIS

Beyond the low-noise comparison in Table 1, we further evaluate **MPU** with extensive experiments on: the number of published noisy copies  $m$ , which measures the computational overhead, and noise level  $\kappa$ . Overall, **MPU** is robust under moderate choices of  $m$ , and  $\kappa$  (Appx.B.6 and Table 2, 3), indicating that **MPU** is tolerable for large noise levels, and few copies is the best choice.

**Number of Copies  $m$**  Table 2 evaluates **MPU** under different numbers of perturbed copies  $m$ . Both computational and communication overheads increase approximately linearly with  $m$ , making it important to examine whether larger copy numbers lead to consistent performance gains. In unlearning settings, the overall computational cost is typically modest, as unlearning is performed for only a few rounds and on

Table 3. Performance comparison of different unlearning algorithms using the **Llama-3.2-1B** model under **MPU** on the TOFU benchmark (Split99), with varying noise levels  $\kappa \in \{0, 0.05, 0.1\}$  and fixed perturbed copies  $m=2$ .

Unlearning Algorithms	Forget Quality $\uparrow$			Forget Truth Ratio $\uparrow$		
	$\kappa=0$	$\kappa=0.05$	$\kappa=0.1$	$\kappa=0$	$\kappa=0.05$	$\kappa=0.1$
GRADASCENT	6.76e-3	<b>0.579</b>	1.43e-2	0.440	<b>0.534</b>	0.430
GRADDIFF	<b>0.405</b>	0.266	0.400	0.546	0.544	<b>0.553</b>
DPO	<b>0.266</b>	0.266	0.165	0.640	0.641	<b>0.637</b>
NPO	<b>0.919</b>	0.919	0.919	0.621	<b>0.624</b>	0.618
SIMNPO	5.41e-2	<b>9.71e-2</b>	5.41e-2	0.520	<b>0.526</b>	0.525
UNDIAL	<b>1.43e-2</b>	1.43e-2	1.43e-2	0.528	<b>0.527</b>	0.526
SATIMP	<b>6.76e-3</b>	3.02e-3	6.76e-3	0.474	<b>0.475</b>	0.475

a relatively small subset of data (e.g., under FORGET01, only 1% of the fine-tuning data is subject to unlearning). As a result, multiplying the computation cost by a factor of  $m$  is generally acceptable when  $m$  is not too large, while it remains preferable to reduce computational overhead by using a smaller  $m$  whenever possible.

We find that **increasing the copy number does not consistently improve unlearning performance, and in some cases can even reduce Forget Quality**. This observation suggests that choosing the minimal setting  $m = 2$  (also the smallest value required to enable denoising aggregation) is sufficient from a performance standpoint, while simultaneously reducing computational and communication overhead. In fact, for certain algorithms, a larger  $m$  can be detrimental. Notably, **GradAscent** improves in FQ when increasing  $m$  from 2 to 3, but collapses at  $m = 4$ , with Model Utility dropping to zero. This behavior indicates that excessively aggressive multi-copy aggregation may distort the effective update direction or amplify instability in the underlying unlearning dynamics for specific methods.

**Noise Level  $\kappa$**  Table 3 studies the effect of the noise magnitude  $\kappa$ . Intuitively,  $\kappa$  serves as a **privacy-perturbation knob**: larger values of  $\kappa$  correspond to stronger parameter perturbations, which enhance privacy protection, but may simultaneously degrade unlearning performance.

Some unlearning methods remain stable across noise levels. For example, **NPO** maintains identical FQ and MU across all tested  $\kappa$  values, and **UNDIAL** exhibits virtually unchanged results as  $\kappa$  increases. This behavior indicates that these algorithms can tolerate relatively large noise without noticeable degradation in FQ or MU.

For noise-sensitive algorithms, a different trend emerges. **GradAscent** improves dramatically at  $\kappa = 0.05$ , achieving its largest FQ and MU among the three settings, but degrades again at  $\kappa = 0.1$ . This pattern is consistent with the view that moderate perturbation can act as an implicit stabilizer (e.g., by smoothing high-variance updates as discussed in Appendix A.6), whereas excessively large noise begins to

distort the effective update signal. Additional analysis of noise-level sensitivity is provided in Appendix B.6.2.

**Increasing Model Size** We further evaluate MPU on a larger base model (Llama-3.2 3B), with results reported in Table 5. We observe that MPU and the noise-free framework achieve nearly identical performance in terms of FQ, FTR, and MU, suggesting that the denoising effect of MPU becomes stronger as the model size increases.

**Round–Epoch Allocation** We examine how the training schedule affects unlearning when the total number of local epochs is fixed in Table 9. Overall, the results indicate a systematic trade-off: using more rounds with fewer local epochs per round tends to improve MU while reducing FQ.

## 5. Conclusion

We propose MPU, a server–client privacy-preserving unlearning framework under a dual non-disclosure constraint: the server does not reveal its exact model parameters, and the client does not share its data. MPU is the first, to our knowledge, to enable unlearning under this strict setting without additional assumptions (e.g., distributional constraints or surrogate models/data), while achieving performance comparable to, and sometimes better than, no-privacy noise-free unlearning. We provide theoretical guarantees that harmonic aggregation eliminates first-order noise error, multi-copy unlearning improves stability, and the reparameterization preserves both functionality and optimization trajectories. Empirically, MPU consistently outperforms privacy baselines and can even surpass the noise-free baseline due to multi-copy stability. Although local computation grows linearly with the copy number, two copies suffice in all our experiments. Future work may design improved communication protocols and further reduce computational cost.

## Impact Statement

This paper presents work whose goal is to advance the field of Machine Learning. There are many potential societal consequences of our work, none of which we feel must be specifically highlighted here.

## References

Bourtoule, L., Chandrasekaran, V., Choquette-Choo, C. A., Jia, H., Travers, A., Zhang, B., Lie, D., and Papernot, N. Machine unlearning. In *2021 IEEE symposium on security and privacy (SP)*, pp. 141–159. IEEE, 2021.

Cao, Y. and Yang, J. Towards making systems forget with machine unlearning. In *2015 IEEE symposium on security and privacy*, pp. 463–480. IEEE, 2015.

Cho, K., van Merriënboer, B., Bahdanau, D., and Bengio, Y. On the properties of neural machine translation: Encoder–decoder approaches. In Wu, D., Carpuat, M., Carreras, X., and Vecchi, E. M. (eds.), *Proceedings of SSST-8, Eighth Workshop on Syntax, Semantics and Structure in Statistical Translation*, pp. 103–111, Doha, Qatar, October 2014. Association for Computational Linguistics. doi: 10.3115/v1/W14-4012. URL <https://aclanthology.org/W14-4012/>.

Dong, Y. R., Lin, H., Belkin, M., Huerta, R., and Vulić, I. Undial: Self-distillation with adjusted logits for robust unlearning in large language models. In *Proceedings of the 2025 Conference of the Nations of the Americas Chapter of the Association for Computational Linguistics: Human Language Technologies (Volume 1: Long Papers)*, pp. 8827–8840, 2025.

Dorna, V., Mekala, A., Zhao, W., McCallum, A., Lipton, Z. C., Kolter, J. Z., and Maini, P. OpenUnlearning: Accelerating LLM unlearning via unified benchmarking of methods and metrics. *arXiv preprint arXiv:2506.12618*, 2025.

Fan, C., Liu, J., Lin, L., Jia, J., Zhang, R., Mei, S., and Liu, S. Simplicity prevails: Rethinking negative preference optimization for llm unlearning. *arXiv preprint arXiv:2410.07163*, 2024.

Ginart, A., Guan, M., Valiant, G., and Zou, J. Y. Making ai forget you: Data deletion in machine learning. *Advances in neural information processing systems*, 32, 2019.

Golatkar, A., Achille, A., and Soatto, S. Eternal sunshine of the spotless net: Selective forgetting in deep networks. In *Proceedings of the IEEE/CVF conference on computer vision and pattern recognition*, pp. 9304–9312, 2020.

Grattafiori, A., Dubey, A., Jauhri, A., Pandey, A., Kadian, A., Al-Dahle, A., Letman, A., Mathur, A., Schelten, A., Vaughan, A., et al. The llama 3 herd of models. *arXiv preprint arXiv:2407.21783*, 2024.

Jang, J., Yoon, D., Yang, S., Cha, S., Lee, M., Logeswaran, L., and Seo, M. Knowledge unlearning for mitigating privacy risks in language models. In *Proceedings of the 61st Annual Meeting of the Association for Computational Linguistics (Volume 1: Long Papers)*, pp. 14389–14408, 2023.

Jin, X., Bu, Z., Vinzamuri, B., Ramakrishna, A., Chang, K.-W., Cevher, V., and Hong, M. Unlearning as multi-task optimization: A normalized gradient difference approach with an adaptive learning rate. In *Proceedings of the 2025 Conference of the Nations of the Americas Chapter of the Association for Computational Linguistics: Human Language Technologies (Volume 1: Long Papers)*, pp. 11278–11294, 2025.

- Koh, P. W. and Liang, P. Understanding black-box predictions via influence functions. In *International conference on machine learning*, pp. 1885–1894. PMLR, 2017.
- Kůrková, V. and Kainen, P. C. Functionally equivalent feedforward neural networks. *Neural Computation*, 6(3): 543–558, 1994.
- Lin, C.-Y. Rouge: A package for automatic evaluation of summaries. In *Text summarization branches out*, pp. 74–81, 2004.
- Liu, B., Liu, Q., and Stone, P. Continual learning and private unlearning. In *Conference on Lifelong Learning Agents*, pp. 243–254. PMLR, 2022a.
- Liu, G., Ma, X., Yang, Y., Wang, C., and Liu, J. Federated unlearning. *arXiv preprint arXiv:2012.13891*, 2020.
- Liu, S., Yao, Y., Jia, J., Casper, S., Baracaldo, N., Hase, P., Yao, Y., Liu, C. Y., Xu, X., Li, H., et al. Rethinking machine unlearning for large language models. *Nature Machine Intelligence*, pp. 1–14, 2025.
- Liu, Y., Xu, L., Yuan, X., Wang, C., and Li, B. The right to be forgotten in federated learning: An efficient realization with rapid retraining. In *IEEE INFOCOM 2022-IEEE conference on computer communications*, pp. 1749–1758. IEEE, 2022b.
- Maini, P., Feng, Z., Schwarzschild, A., Lipton, Z. C., and Kolter, J. Z. Tofu: A task of fictitious unlearning for llms. *arXiv preprint arXiv:2401.06121*, 2024.
- Mekala, A. R., Dorna, V., Dubey, S., Lalwani, A., Koleczek, D., Rungta, M., Hasan, S. A., and Lobo, E. A. Alternate preference optimization for unlearning factual knowledge in large language models. In *Proceedings of the 31st International Conference on Computational Linguistics*, pp. 3732–3752, 2025.
- Mironov, I. Rényi differential privacy. In *IEEE Computer Security Foundations Symposium (CSF)*, 2017.
- Pan, Z., Zhang, S., Zheng, Y., Li, C., Cheng, Y., and Zhao, J. Multi-objective large language model unlearning. In *ICASSP 2025-2025 IEEE International Conference on Acoustics, Speech and Signal Processing (ICASSP)*, pp. 1–5. IEEE, 2025.
- Qiu, R., Tan, J., Pu, J., Wang, H., Gao, X.-S., and Sun, F. A survey on unlearning in large language models. *arXiv preprint arXiv:2510.25117*, 2025.
- Qwen, A. Y., Yang, B., Zhang, B., Hui, B., Zheng, B., Yu, B., Li, C., Liu, D., Huang, F., Wei, H., et al. Qwen2. 5 technical report. *arXiv preprint*, 2024.
- Rafailov, R., Sharma, A., Mitchell, E., Manning, C. D., Ermon, S., and Finn, C. Direct preference optimization: Your language model is secretly a reward model. *Advances in neural information processing systems*, 36: 53728–53741, 2023.
- Shen, W. F., Qiu, X., Kurmanji, M., Iacob, A., Sani, L., Chen, Y., Cancedda, N., and Lane, N. D. Lunar: Llm unlearning via neural activation redirection. *arXiv preprint arXiv:2502.07218*, 2025.
- Vaswani, A., Shazeer, N., Parmar, N., Uszkoreit, J., Jones, L., Gomez, A. N., Kaiser, Ł., and Polosukhin, I. Attention is all you need. *Advances in neural information processing systems*, 30, 2017.
- Wang, B., Zi, Y., Sun, Y., Zhao, Y., and Qin, B. Balancing forget quality and model utility: A reverse kl-divergence knowledge distillation approach for better unlearning in llms. In *Proceedings of the 2025 Conference of the Nations of the Americas Chapter of the Association for Computational Linguistics: Human Language Technologies (Volume 1: Long Papers)*, pp. 1306–1321, 2025.
- Wang, Y., Wei, J., Liu, C. Y., Pang, J., Liu, Q., Shah, A. P., Bao, Y., Liu, Y., and Wei, W. LLM unlearning via loss adjustment with only forget data. *arXiv preprint arXiv:2410.11143*, 2024.
- Wortsman, M., Ilharco, G., Gadre, S. Y., Roelofs, R., Gontijo-Lopes, R., Morcos, A. S., Namkoong, H., Farhadi, A., Carmon, Y., Kornblith, S., et al. Model soups: averaging weights of multiple fine-tuned models improves accuracy without increasing inference time. In *International conference on machine learning*, pp. 23965–23998. PMLR, 2022.
- Yang, P., Wang, Q., Huang, Z., Liu, T., Zhang, C., and Han, B. Exploring criteria of loss reweighting to enhance llm unlearning. *arXiv preprint arXiv:2505.11953*, 2025.
- Yao, Y., Xu, X., and Liu, Y. Large language model unlearning. *Advances in Neural Information Processing Systems*, 37:105425–105475, 2024.
- Zhang, F., Yan, X., Wu, T., Li, W., Chen, T., Cao, Y., Yan, R., Huang, L., Lim, W. Y. B., and Yang, Q. Oblivionis: A lightweight learning and unlearning framework for federated large language models. *arXiv preprint arXiv:2508.08875*, 2025.
- Zhang, R., Lin, L., Bai, Y., and Mei, S. Negative preference optimization: From catastrophic collapse to effective unlearning. *arXiv preprint arXiv:2404.05868*, 2024.
- Zhou, Y., Song, L., Wang, B., and Chen, W. Metagpt: Merging large language models using model exclusive task arithmetic. *arXiv preprint arXiv:2406.11385*, 2024a.

Zhou, Z., Chen, Z., Chen, Y., Zhang, B., and Yan, J. On the emergence of cross-task linearity in the pretraining-finetuning paradigm. *arXiv preprint arXiv:2402.03660*, 2024b.

## Appendix Overview

This appendix provides supplementary materials for MPU that expand the main paper along two axes: (i) mathematical derivations and analysis supporting the core design (noise construction, denoising aggregation, and function-preserving reparameterizations), and (ii) experimental details, evaluation, additional results, and ablations.

To keep the appendix navigable, we organize it into two parts.

**Part A: Mathematical Details and Analysis** This part provides the mathematical foundations behind MPU, including the structured zero-sum noise, harmonic denoising aggregation, Transformer reparameterization symmetries, and a formal comparison against a naive single-copy “noise-only” baseline.

- **Appendix A.1:** Structured zero-sum noise construction and statistics, including marginal variance, cross-covariance, and the stacked covariance form.
- **Appendix A.2:** Harmonic denoising aggregation, including first-order exact cancellation, second-order remainder bounds (Appx. A.2.2), and the uniqueness/optimalty of harmonic weights (Appx. A.2.3).
- **Appendix A.3:** Function-preserving reparameterizations for Transformers, including attention head basis transforms (Appx. A.3.1), RoPE-aware commutant restrictions (Appx. A.3.2), Feed-Forward Neural Network hidden-channel permutations (Appx. A.3.3), and linearity of the reparameterization map (Appx. A.3.4).
- **Appendix A.4:** Discussion of whether reparameterization affects client-side optimization trajectories and loss smoothness (equivariance and Euclidean smoothness invariance).
- **Appendix A.5:** Comparison of update error between MPU and single-copy noisy unlearning, including one-round bias and variance analysis (Appx. A.5.1), multi-round implications (Appx. A.5.2), and an SNR interpretation (Appx. A.5.3).
- **Appendix A.6:** Method discussion on stability enhancement via multi-copy learning.

**Part B: Implementation Details and Supplementary Experiments** This part provides benchmark descriptions, evaluation metrics, unlearning algorithm formulations, implementation details, and extensive supplementary experiments and ablations.

- **Appendix B.1:** Benchmark description.
- **Appendix B.2:** Evaluation metrics, including memorization (Appx. B.2.1), privacy (Appx. B.2.2), and utility (Appx. B.2.3).
- **Appendix B.3:** Unlearning algorithms instantiated within MPU.
- **Appendix B.4:** Implementation details, including testbed configuration (Appx. B.4.1), default hyperparameters (Appx. B.4.2), and the prompt template used for training and evaluation (Appx. B.4.3).
- **Appendix B.5:** Additional experimental results.
- **Appendix B.6:** Detailed supplementary analysis and ablations, including the effect of copy number  $m$  (Appx. B.6.1), noise level  $\kappa$  (Appx. B.6.2), round–epoch allocation (Appx. B.6.3), the no-denoise ablation (Appx. B.6.4), robustness to larger forget splits (Appx. B.6.5), and scaling across model sizes (Appx. B.6.6).

## A. Mathematical Details and Analysis

This appendix provides the mathematical details supporting the method described in Sec. 3, including: (i) the structured zero-sum noise construction (Sec. 3.2.1), (ii) the harmonic denoising aggregation and its associated error terms (Sec. 3.4), and (iii) the function-preserving reparameterization family used to obfuscate the original parameter space (Sec. 3.2.2). We additionally present a comparison with a naive single-copy “noise-only” baseline, which injects noise but performs no denoising.

### A.1. Structured Zero-Sum Noise Construction and Statistics

Fix a communication round  $r$  and a parameter block (e.g., a layer)  $\ell$  with dimension  $d_\ell$ . Recall the construction in Eq. (2): draw i.i.d.  $z_{k,\ell}^{(r)} \sim \mathcal{N}(0, \sigma_\ell^2 I_{d_\ell})$  for  $k \in [m]$ , define  $\bar{z}_\ell^{(r)} = \frac{1}{m} \sum_{k=1}^m z_{k,\ell}^{(r)}$ , and set

$$\epsilon_{k,\ell}^{0,(r)} = \sqrt{\frac{m}{m-1}} \left( z_{k,\ell}^{(r)} - \bar{z}_\ell^{(r)} \right), \quad \epsilon_{k,\ell}^{(r)} = \alpha_k \epsilon_{k,\ell}^{0,(r)}. \quad (19)$$

By construction,  $\sum_{k=1}^m \epsilon_{k,\ell}^{0,(r)} \equiv 0$  for every block  $\ell$ , and hence  $\sum_k \epsilon_k^{0,(r)} \equiv 0$  for the stacked vector.

We define

$$\epsilon_k^{0,(r)} = \text{stack}_\ell(\epsilon_{k,\ell}^{0,(r)}), \quad (20)$$

where the stack operation means to stack the block-wise noises together to obtain a model-level noise.

**Marginal Distribution and Cross-Covariance of Zero-Sum Base** Let  $z_k := z_{k,\ell}^{(r)} \in \mathbb{R}^{d_\ell}$  and  $\bar{z} = \frac{1}{m} \sum_{k=1}^m z_k$ . Since  $z_k \sim \mathcal{N}(0, \sigma_\ell^2 I_{d_\ell})$  are i.i.d., we have

$$\text{Var}(z_k - \bar{z}) = \left(1 - \frac{1}{m}\right) \sigma_\ell^2 I_{d_\ell}. \quad (21)$$

The scaling factor  $\sqrt{\frac{m}{m-1}}$  therefore restores the desired marginal variance:

$$\text{Var}(\epsilon_{k,\ell}^{0,(r)}) = \frac{m}{m-1} \text{Var}(z_k - \bar{z}) = \sigma_\ell^2 I_{d_\ell} \Rightarrow \epsilon_{k,\ell}^{0,(r)} \sim \mathcal{N}(0, \sigma_\ell^2 I_{d_\ell}) \text{ marginally}. \quad (22)$$

For  $k \neq j$ , using  $\text{Cov}(z_k, \bar{z}) = \frac{1}{m} \sigma_\ell^2 I_{d_\ell}$  and  $\text{Var}(\bar{z}) = \frac{1}{m} \sigma_\ell^2 I_{d_\ell}$ , we obtain

$$\text{Cov}(z_k - \bar{z}, z_j - \bar{z}) = -\frac{1}{m} \sigma_\ell^2 I_{d_\ell}, \quad (23)$$

and hence, after scaling,

$$\text{Cov}(\epsilon_{k,\ell}^{0,(r)}, \epsilon_{j,\ell}^{0,(r)}) = -\frac{1}{m-1} \sigma_\ell^2 I_{d_\ell}, \quad k \neq j. \quad (24)$$

After applying the per-copy scaling, this becomes

$$\text{Cov}(\epsilon_{k,\ell}^{(r)}, \epsilon_{j,\ell}^{(r)}) = -\frac{\alpha_k \alpha_j}{m-1} \sigma_\ell^2 I_{d_\ell}, \quad k \neq j. \quad (25)$$

**Scaled-Copy Covariance (Matrix Form)** Let  $\epsilon_\ell := [\epsilon_{1,\ell}^{(r)}; \dots; \epsilon_{m,\ell}^{(r)}] \in \mathbb{R}^{md_\ell}$  be the stacked noise vector for block  $\ell$ . Then

$$\text{Cov}[\epsilon_\ell] = \sigma_\ell^2 (DBD) \otimes I_{d_\ell}, \quad (26)$$

where

$$D = \text{diag}(\alpha_1, \dots, \alpha_m), \quad B = \frac{m}{m-1} I_m - \frac{1}{m-1} \mathbf{1}\mathbf{1}^\top. \quad (27)$$

Since  $B$  has eigenvalues  $\frac{m}{m-1}$  (multiplicity  $m-1$ ) and 0 (multiplicity 1),  $\text{Cov}[\epsilon_\ell]$  has rank  $(m-1)d_\ell$ . This expresses the core property used by harmonic denoising: the  $m$  copy noises live in an  $(m-1)$ -dimensional subspace (per block), and the “missing” direction is precisely the all-ones direction that harmonic aggregation cancels.

## A.2. Harmonic Denoising Aggregation: Cancellation, Remainder, and Streaming

We (i) formalize the first-order cancellation argument, (ii) derive a clean second-order remainder bound under a local smoothness assumption, (iii) establish the uniqueness and optimality of harmonic weights for zero-sum cancellation, and (iv) justify the streaming implementation used by MPU (Sec. 3.5).

**Local Linearization Model** Let  $\Delta^*(\theta)$  denote the ideal (noise-free) unlearning displacement produced by the chosen unlearning trainer when initialized at parameters  $\theta$ . For analytical clarity, we assume fixed client data and fixed algorithmic randomness. Define the Jacobian of  $\Delta^*$  at the current iterate as

$$J = \left. \frac{\partial \Delta^*(\theta)}{\partial \theta} \right|_{\theta_{r-1}}. \quad (28)$$

After inverting the reparameterization (Sec. 3.4), we model each aligned update via a first-order expansion in the injected perturbation:

$$\widehat{\Delta}^{(k,r)} = \Delta^*(\theta_{r-1}) + J \epsilon_k^{(r)} + \rho_k^{(r)}, \quad \epsilon_k^{(r)} = \alpha_k \epsilon_k^{0,(r)}, \quad (29)$$

where the remainder term  $\rho_k^{(r)}$  captures second-order (and higher-order) effects, as well as any deviation from modeling the client-side unlearning routine as a deterministic map.

### A.2.1. FIRST-ORDER EXACT CANCELLATION VIA HARMONIC WEIGHTS

The server aggregates the aligned updates using harmonic weights  $w_k \propto \alpha_k^{-1}$ :

$$\bar{\Delta}^{(r)} = \sum_{k=1}^m w_k \widehat{\Delta}^{(k,r)}, \quad w_k := \frac{\alpha_k^{-1}}{\sum_{j=1}^m \alpha_j^{-1}}. \quad (30)$$

Substituting the first-order model in Eq. (29) yields

$$\bar{\Delta}^{(r)} = \Delta^*(\theta_{r-1}) + J \sum_{k=1}^m w_k \epsilon_k^{(r)} + \sum_{k=1}^m w_k \rho_k^{(r)}. \quad (31)$$

Since

$$w_k \epsilon_k^{(r)} = \frac{\alpha_k^{-1}}{S_0} \alpha_k \epsilon_k^{0,(r)} = \frac{1}{S_0} \epsilon_k^{0,(r)}, \quad S_0 := \sum_{j=1}^m \alpha_j^{-1}, \quad (32)$$

we obtain

$$\sum_{k=1}^m w_k \epsilon_k^{(r)} = \frac{1}{S_0} \sum_{k=1}^m \epsilon_k^{0,(r)} = 0, \quad (33)$$

where the last equality follows from the zero-sum property in Eq. (2).

Therefore,

$$\bar{\Delta}^{(r)} = \Delta^*(\theta_{r-1}) + \sum_{k=1}^m w_k \rho_k^{(r)}, \quad (34)$$

which formally establishes that the injected noise is canceled *exactly to first order*.

### A.2.2. SECOND-ORDER REMAINDER UNDER LIPSCHITZ JACOBIAN

A standard approach to control the remainder term  $\rho_k^{(r)}$  is to assume local smoothness of the Jacobian.

**Assumption (Local Lipschitz Jacobian)** Assume that  $\Delta^*(\theta)$  is Fréchet differentiable in a neighborhood of  $\theta_{r-1}$ , and that its Jacobian  $J(\theta)$  is  $L_J$ -Lipschitz in this neighborhood:

$$\|J(\theta) - J(\theta')\| \leq L_J \|\theta - \theta'\|. \quad (35)$$

**Remainder Bound** Let  $\delta_k^{(r)} := \epsilon_k^{(r)}$ . By the integral remainder form of Taylor’s theorem, we have

$$\begin{aligned}\rho_k^{(r)} &= \Delta^*(\theta_{r-1} + \delta_k^{(r)}) - \Delta^*(\theta_{r-1}) - J \delta_k^{(r)} \\ &= \int_0^1 \left( J(\theta_{r-1} + t \delta_k^{(r)}) - J(\theta_{r-1}) \right) \delta_k^{(r)} dt.\end{aligned}\quad (36)$$

Taking norms and applying the Lipschitz condition yields

$$\|\rho_k^{(r)}\| \leq \int_0^1 L_J t \|\delta_k^{(r)}\|^2 dt = \frac{L_J}{2} \|\epsilon_k^{(r)}\|^2. \quad (37)$$

Consequently,

$$\|\bar{\Delta}^{(r)} - \Delta^*(\theta_{r-1})\| = \left\| \sum_{k=1}^m w_k \rho_k^{(r)} \right\| \leq \frac{L_J}{2} \sum_{k=1}^m w_k \|\epsilon_k^{(r)}\|^2, \quad (38)$$

which matches the  $O(\|\epsilon\|^2)$  behavior stated in Sec. 3.4.

### A.2.3. UNIQUENESS AND OPTIMALITY OF HARMONIC WEIGHTS

In this section, we show that harmonic weights are the unique linear weights that cancel the first-order perturbation for *all* zero-sum noise realizations.

**Proposition A.1** (Uniqueness of Harmonic Weights for Zero-Sum Cancellation). *Consider a linear estimator of the form  $\sum_{k=1}^m w_k \hat{\Delta}^{(k,r)}$  with  $\sum_{k=1}^m w_k = 1$ . Assume the linear response model*

$$\hat{\Delta}^{(k,r)} = \Delta^*(\theta_{r-1}) + J \alpha_k \epsilon_k^{0,(r)} + \rho_k^{(r)}, \quad (39)$$

where the base noises satisfy  $\sum_{k=1}^m \epsilon_k^{0,(r)} \equiv 0$ . If the first-order term cancels for all such zero-sum realizations, i.e.,

$$\sum_{k=1}^m w_k \alpha_k \epsilon_k^{0,(r)} \equiv 0 \quad \text{for all } \{\epsilon_k^{0,(r)}\}_{k=1}^m \text{ with } \sum_{k=1}^m \epsilon_k^{0,(r)} = 0, \quad (40)$$

then necessarily

$$w_k = \frac{\alpha_k^{-1}}{\sum_{j=1}^m \alpha_j^{-1}}, \quad k = 1, \dots, m. \quad (41)$$

*Proof.* Cancellation for all zero-sum realizations is equivalent to requiring that the vector  $(w_k \alpha_k)_{k=1}^m$  is orthogonal to the entire subspace  $\{\epsilon_k \in \mathbb{R}^m : \sum_{k=1}^m \epsilon_k = 0\}$ . This subspace is spanned by pairwise difference vectors of the form  $e_i - e_j$ . Hence, orthogonality implies  $w_i \alpha_i = w_j \alpha_j$  for all  $i, j$ , i.e.,  $w_k \alpha_k = c$  for some constant  $c$ . Imposing the normalization  $\sum_{k=1}^m w_k = 1$  yields  $c = 1/\sum_{j=1}^m \alpha_j^{-1}$ , which gives the harmonic form.  $\square$

**Variance Reduction of Client-Side Randomness** Suppose the aligned updates additionally include zero-mean stochasticity from local training,

$$\hat{\Delta}^{(k,r)} = \Delta^*(\theta_{r-1}) + J \epsilon_k^{(r)} + \eta_k^{(r)} + \rho_k^{(r)}, \quad (42)$$

where  $\mathbb{E}[\eta_k^{(r)}] = 0$  and  $\text{Cov}(\eta_k^{(r)}) = \Sigma_\eta$ , independently across  $k$ . Ignoring the  $O(\|\epsilon\|^2)$  remainder terms for clarity, the covariance of the aggregated update satisfies

$$\text{Cov}(\bar{\Delta}^{(r)}) = \sum_{k=1}^m w_k^2 \Sigma_\eta = \left( \frac{\sum_{k=1}^m \alpha_k^{-2}}{(\sum_{k=1}^m \alpha_k^{-1})^2} \right) \Sigma_\eta. \quad (43)$$

When the scales  $\{\alpha_k\}$  are of comparable magnitude, the prefactor scales as  $\asymp 1/m$ , formalizing the  $1/m$  variance-reduction intuition discussed in Sec. A.6.

### A.3. Function-Preserving Reparameterizations

This section expands Sec. 3.2.2 by providing full Transformer-level details. We describe the reparameterizations used by MPU from a group-theoretic perspective and present explicit forward and inverse formulas together with invariance proofs, including the RoPE-commutation constraint.

**Parameter-Symmetry Group Viewpoint** Let  $\Theta$  denote the parameter tuple of a Transformer block, and let  $f_\Theta : \mathbb{R}^{L \times d_{\text{model}}} \rightarrow \mathbb{R}^{L \times d_{\text{model}}}$  denote the forward function induced by  $\Theta$  on a length- $L$  sequence. Define the set of *function-preserving reparameterizations* as

$$\mathcal{G} = \left\{ T : \Theta \mapsto T(\Theta) \mid T \text{ is invertible and } f_{T(\Theta)}(X) = f_\Theta(X) \forall X \right\}. \quad (44)$$

Under composition,  $\mathcal{G}$  forms a group, and each  $T \in \mathcal{G}$  constitutes a parameter-symmetry of the model.

In MPU, we take  $L = d_{\text{ff}}$  and sample  $T_{k,r}$  *data-independently* from a structured subset  $\mathcal{T} \subseteq \mathcal{G}$  constructed from: (i) discrete channel permutations within FFN submodules, and (ii) continuous orthogonal basis changes within attention head subspaces. For RoPE-based models, we further restrict the attention basis changes to lie in the commutant of the RoPE operators, ensuring functional invariance.

#### A.3.1. ATTENTION HEAD REPARAMETERIZATION

**Shapes** Let  $d_{\text{model}}$  denote the model width,  $d_h$  the head dimension,  $H_Q$  the number of query heads, and  $H_{KV}$  the number of key/value heads (GQA/MQA are covered by  $H_Q \geq H_{KV}$ ). We use the following parameter shapes:

$$W_Q \in \mathbb{R}^{d_{\text{model}} \times (H_Q d_h)}, \quad (45a)$$

$$W_K, W_V \in \mathbb{R}^{d_{\text{model}} \times (H_{KV} d_h)}, \quad (45b)$$

$$W_O \in \mathbb{R}^{(H_Q d_h) \times d_{\text{model}}}. \quad (45c)$$

**Group Element and Lifted Action** Let  $\pi : [H_Q] \rightarrow [H_{KV}]$  denote the fixed assignment mapping each query head to its corresponding key/value head. Sample per-KV orthogonal blocks  $S_j \in O(d_h)$  for  $j = 1, \dots, H_{KV}$ , and define

$$S_{KV} := \text{diag}(S_1, \dots, S_{H_{KV}}) \in O(H_{KV} d_h), \quad (46a)$$

$$U(\pi, S_{KV}) := \text{blkdiag}(S_{\pi(1)}, \dots, S_{\pi(H_Q)}) \in O(H_Q d_h). \quad (46b)$$

Both  $S_{KV}$  and  $U(\pi, S_{KV})$  are orthogonal matrices.

**Forward and Inverse Formulas** The reparameterization acts on the attention weights as

$$W'_Q = W_Q U(\pi, S_{KV}), \quad W'_K = W_K S_{KV}, \quad (47a)$$

$$W'_V = W_V S_{KV}, \quad W'_O = U(\pi, S_{KV})^\top W_O. \quad (47b)$$

If biases are present, apply the same right-multiplication:  $b'_Q = b_Q U(\pi, S_{KV})$ ,  $b'_K = b_K S_{KV}$ , and  $b'_V = b_V S_{KV}$ . The inverse transformation is given by transposition:

$$W_Q = W'_Q U(\pi, S_{KV})^\top, \quad W_K = W'_K S_{KV}^\top, \quad (48a)$$

$$W_V = W'_V S_{KV}^\top, \quad W_O = U(\pi, S_{KV}) W'_O. \quad (48b)$$

**Function Invariance (without RoPE)** Let  $X \in \mathbb{R}^{L \times d_{\text{model}}}$  and define  $Q = XW_Q$ ,  $K = XW_K$ , and  $V = XW_V$ , with head-wise partitions  $Q = [Q_1 \mid \dots \mid Q_{H_Q}]$ ,  $K = [K_1 \mid \dots \mid K_{H_{KV}}]$ , and  $V = [V_1 \mid \dots \mid V_{H_{KV}}]$ , where each  $Q_i, K_j, V_j \in \mathbb{R}^{L \times d_h}$ . For GQA attention, the outputs are given by

$$A_i = \text{softmax}\left(\frac{1}{\sqrt{d_h}} Q_i K_{\pi(i)}^\top\right), \quad O_i = A_i V_{\pi(i)}, \quad Y = [O_1 \mid \dots \mid O_{H_Q}] W_O. \quad (49)$$

**Claim** Under the reparameterization in Eq. (47), the realized attention function is invariant, i.e.,  $Y' = Y$ .

*Proof.* From Eq. (47), we have  $Q' = QU(\pi, S_{KV})$  and  $K' = KS_{KV}$ ,  $V' = VS_{KV}$ . Consequently,  $Q'_i = Q_i S_{\pi(i)}$  and  $K'_{\pi(i)} = K_{\pi(i)} S_{\pi(i)}$ . Since  $S_{\pi(i)}^\top S_{\pi(i)} = I$ , it follows that

$$Q'_i K'_{\pi(i)\top} = (Q_i S_{\pi(i)}) (S_{\pi(i)}^\top K_{\pi(i)}^\top) = Q_i K_{\pi(i)}^\top, \quad (50)$$

and hence the attention logits, and therefore  $A'_i$ , are unchanged.

Moreover,

$$O'_i = A'_i V'_{\pi(i)} = A_i (V_{\pi(i)} S_{\pi(i)}) = (O_i) S_{\pi(i)}. \quad (51)$$

Concatenation yields  $[O'_1 | \dots | O'_{H_Q}] = [O_1 | \dots | O_{H_Q}] U(\pi, S_{KV})$ . Finally, using  $W'_O = U(\pi, S_{KV})^\top W_O$ , we obtain

$$Y' = [O'] W'_O = ([O] U) (U^\top W_O) = [O] W_O = Y, \quad (52)$$

which completes the proof.  $\square$

### A.3.2. ROPE-AWARE SPECIALIZATION (COMMUTANT RESTRICTION)

Llama-type decoders apply rotary positional embeddings (RoPE) to queries and keys via right-multiplication by a position-dependent orthogonal operator  $\Phi(p) \in \mathbb{R}^{d_h \times d_h}$ :

$$\tilde{Q}_i[p, :] = Q_i[p, :] \Phi(p)^\top, \quad \tilde{K}_j[p, :] = K_j[p, :] \Phi(p)^\top. \quad (53)$$

RoPE acts as independent  $2 \times 2$  rotations on  $d_h/2$  disjoint planes,

$$\Phi(p) = \text{blkdiag}(R(\omega_1 p), \dots, R(\omega_{d_h/2} p)), \quad R(\varphi) = \begin{bmatrix} \cos \varphi & -\sin \varphi \\ \sin \varphi & \cos \varphi \end{bmatrix} \in \text{SO}(2). \quad (54)$$

To preserve the attention logits, we require the head-basis transform to commute with all  $\Phi(p)$ , i.e.,

$$S_j \Phi(p) = \Phi(p) S_j, \quad \forall p. \quad (55)$$

**Commutant under Distinct Frequencies** When the RoPE frequencies  $\{\omega_r\}$  are distinct across the  $d_h/2$  planes, the orthogonal transformations that commute with all  $\Phi(p)$  are exactly the per-plane rotations:

$$S_j = \text{blkdiag}(R(\varphi_{j,1}), \dots, R(\varphi_{j,d_h/2})) \in \text{SO}(2)^{d_h/2}, \quad j = 1, \dots, H_{KV}. \quad (56)$$

Reflections in  $O(2)^{d_h/2} \setminus \text{SO}(2)^{d_h/2}$  generally fail to commute with  $\Phi(p)$ , except at degenerate angles. The rotation angles  $\{\varphi_{j,r}\}$  may be sampled deterministically from the round seed and indices  $(t_r, k, \text{layer}, j, r)$ .

**Function Invariance with RoPE** Under the commutation condition  $S_{\pi(i)} \Phi(p) = \Phi(p) S_{\pi(i)}$ , the proof of function invariance follows identically to the non-RoPE case. In particular, commutativity implies

$$S_{\pi(i)} \Phi(p)^\top \Phi(p') S_{\pi(i)}^\top = \Phi(p)^\top \Phi(p'), \quad (57)$$

inside the attention logits, so the attention weights remain unchanged. The output invariance then follows as before via cancellation with  $W'_O = U(\pi, S_{KV})^\top W_O$ .

### A.3.3. FEED-FORWARD BLOCKS: HIDDEN-CHANNEL PERMUTATIONS

**Standard Two-Layer Feed-Forward Neural Network** Consider an FFN with parameters  $(W_1, b_1, W_2, b_2)$  and an element-wise nonlinearity  $\sigma$ :

$$f_\Theta(x) = W_2 \sigma(W_1 x + b_1) + b_2. \quad (58)$$

Let  $P \in \mathbb{R}^{d_{\text{ff}} \times d_{\text{ff}}}$  be a permutation matrix ( $P^{-1} = P^\top$ ) acting on hidden channels. Define the reparameterization

$$W'_1 = P W_1, \quad b'_1 = P b_1, \quad W'_2 = W_2 P^\top, \quad b'_2 = b_2. \quad (59)$$

Since element-wise activations are permutation-equivariant, i.e.,  $\sigma(Pz) = P\sigma(z)$ , we have

$$\begin{aligned} W'_2\sigma(W'_1x + b'_1) + b'_2 &= W_2P^\top\sigma(P(W_1x + b_1)) + b_2 \\ &= W_2P^\top P\sigma(W_1x + b_1) + b_2 \\ &= f_\Theta(x). \end{aligned} \tag{60}$$

Thus, hidden-channel permutations are function-preserving, matching the group action in Eq. (8) in the main text.

**SwiGLU/GEGLU-Style Gated Feed-Forward Neural Networks** Modern LLMs (e.g., the Llama 3.2 family) employ gated FFNs such as SwiGLU. For gated architectures with *gate* and *up* branches combined via an element-wise product, the same permutation must be applied to both branches to preserve consistency.

Concretely, for parameters  $(W_{1,\text{gate}}, W_{1,\text{up}}, b_1, W_2, b_2)$ , define

$$W'_{1,\text{gate}} = PW_{1,\text{gate}}, \quad W'_{1,\text{up}} = PW_{1,\text{up}}, \quad b'_1 = Pb_1, \quad W'_2 = W_2P^\top, \quad b'_2 = b_2. \tag{61}$$

Permutation-equivariance together with  $P^\top((Pa) \odot (Pb)) = a \odot b$  ensures functional invariance.

#### A.3.4. LINEARITY OF REPARAMETERIZATION MAP

In **MPU**, each  $T_{k,r}$  is implemented via multiplication by orthogonal or permutation matrices acting on parameter tensors (through left/right multiplication and block-diagonal composition). Consequently,  $T_{k,r}$  is a *linear isomorphism* on the parameter space. For conformable parameter collections  $a, b$  and any scalar  $c$ ,

$$T(a + b) = T(a) + T(b), \quad T(ca) = cT(a), \quad T^{-1} \text{ exists and is linear.} \tag{62}$$

This property justifies applying  $T_{k,r}^{-1}$  directly to the returned parameter updates in Algorithm 1. Specifically, if the client returns a displacement in the transformed coordinates, mapping it back via  $T^{-1}$  yields the corresponding displacement in the canonical coordinates:

$$T^{-1}(T(\theta) + \eta \Delta(T(\theta))) = \theta + \eta T^{-1}(\Delta(T(\theta))). \tag{63}$$

#### A.4. Discussion: Effects of Reparameterization on Optimization Trajectory and Smoothness

A natural concern is whether the client-side reparameterization introduced in Sec. 3.2.2 (and Appendix A.3) alters the optimization dynamics of local unlearning. We address two questions: *(i)* when the optimization trajectory is *equivariant* under the reparameterization, and *(ii)* whether the reparameterization can change the apparent smoothness of the loss landscape.

**Setup** Let  $\mathcal{U}(\theta)$  denote the client-side unlearning objective (e.g., the loss used by GradAscent, NPO, or GradDiff) as a function of the model parameters  $\theta \in \mathbb{R}^d$ . For a function-preserving reparameterization  $T \in \mathcal{T}$  (Sec. 3.2.2), we have  $f_{T(\theta)}(\cdot) \equiv f_\theta(\cdot)$  and therefore, for any objective depending only on model outputs,

$$\mathcal{U}(T(\theta)) = \mathcal{U}(\theta). \tag{64}$$

In **MPU**, each  $T_{k,r}$  is implemented via orthogonal or permutation actions on weight matrices (Appendix A.3). Viewed as a linear map on the vectorized parameter space, this implies that  $T$  is an *isometry*:

$$\langle Ta, Tb \rangle = \langle a, b \rangle, \quad \|Ta\|_2 = \|a\|_2, \quad T^{-1} = T^\top. \tag{65}$$

##### A.4.1. EQUIVARIANCE OF GRADIENT DESCENT UNDER ORTHOGONAL OR PERMUTATION REPARAMETERIZATIONS

Define the reparameterized objective  $\mathcal{U}_T(\vartheta) := \mathcal{U}(T^{-1}\vartheta)$  in the published coordinates  $\vartheta = T(\theta)$ . By the chain rule together with Eq. (65),

$$\nabla_{\vartheta}\mathcal{U}_T(\vartheta) = T\nabla_{\theta}\mathcal{U}(\theta), \quad \theta = T^{-1}\vartheta. \tag{66}$$

Consider  $t$  steps of (stochastic) gradient descent in the published coordinates:

$$\vartheta_{s+1} = \vartheta_s - \eta g_s(\vartheta_s), \tag{67}$$

where  $g_s(\vartheta_s)$  is an unbiased estimator of  $\nabla_{\vartheta} \mathcal{U}_T(\vartheta_s)$  (e.g., mini-batch SGD). Mapping back via  $\theta_s := T^{-1}\vartheta_s$  and using Eq. (66) yields

$$\theta_{s+1} = T^{-1}\vartheta_{s+1} = \theta_s - \eta T^{-1}g_s(\vartheta_s) \approx \theta_s - \eta \nabla_{\theta} \mathcal{U}(\theta_s), \quad (68)$$

i.e., the mapped-back iterates follow the same optimization trajectory as if the client had optimized directly in the canonical coordinates from the corresponding initialization. This equivariance holds *exactly* for deterministic gradient descent, and holds in distribution for SGD under the natural coupling in which the same mini-batches are used and the stochastic gradients are transformed consistently by  $T$ . The argument also extends to common modifications such as momentum and  $\ell_2$  weight decay, since Eq. (65) preserves the Euclidean norm.

#### A.4.2. INVARIANCE OF EUCLIDEAN SMOOTHNESS

Because  $T$  is an orthogonal or permutation change of coordinates, it does *not* alter curvature measured under the Euclidean metric. Let  $H(\theta) := \nabla_{\theta}^2 \mathcal{U}(\theta)$  and  $H_T(\vartheta) := \nabla_{\vartheta}^2 \mathcal{U}_T(\vartheta)$ . Differentiating Eq. (66) yields the similarity relation

$$H_T(\vartheta) = T H(\theta) T^{\top}, \quad \theta = T^{-1}\vartheta. \quad (69)$$

Consequently, the Hessian spectrum is preserved:  $\lambda_{\max}(H_T(\vartheta)) = \lambda_{\max}(H(\theta))$ , and likewise for the operator norm  $\|H_T\|_2$ . Equivalently, if  $\mathcal{U}$  is  $L$ -smooth in  $\theta$  (i.e., its gradient is  $L$ -Lipschitz), then  $\mathcal{U}_T$  is also  $L$ -smooth in  $\vartheta$ . Thus, under Euclidean geometry, the reparameterization does *not* make the loss landscape appear smoother or sharper; it merely rotates or permutes the coordinate axes within a functionally equivalent parameter orbit.

### A.5. Comparison of Update Error: MPU vs. Single-Copy Noisy Unlearning

In this section, we compare **MPU** with a noise-injection baseline that performs no denoising, which serves as a controlled reference for isolating the effect of our denoising mechanism.

To ensure a fair comparison between **MPU** and the NOISED baseline, we scale the noise parameter  $\kappa$  of the NOISED baseline by the expected value of the scaling factor in **MPU**. As a result, the noise level of the NOISED baseline matches the average noise level across multiple copies in **MPU**.

**Baseline (Noise-Only, No Denoising)** Define a single-copy procedure that, in each round  $r$ : **(i)** samples a noise vector  $\varepsilon^{(r)}$  with the same block-wise scales as **MPU** (e.g.,  $\varepsilon_{\ell}^{(r)} \sim \mathcal{N}(0, \sigma_{\ell}^2 I_{d_{\ell}})$ ) and overall scale matched to  $\mathbb{E}_k(\alpha_k)$ ; **(ii)** publishes  $\theta_{r-1} + \varepsilon^{(r)}$  to the client; **(iii)** runs local unlearning from this noisy initialization; and **(iv)** uses the resulting parameters as the next-round model.

Let the unlearning routine induce a displacement map  $\Delta(\theta)$  so that the updated parameters are  $\theta + \Delta(\theta)$ . The baseline state evolution is

$$\theta_r^{\text{NO}} = \theta_{r-1}^{\text{NO}} + \varepsilon^{(r)} + \eta_{\text{srv}} \Delta\left(\theta_{r-1}^{\text{NO}} + \varepsilon^{(r)}\right), \quad (70)$$

where  $\eta_{\text{srv}}$  matches the server step size in Algorithm 1.

**Linear Response Model** Fix an anchor point  $\theta$  (e.g.,  $\theta = \theta_{r-1}$ ) and write the perturbation as  $u$ . Under the same local linearization used in Sec. 3.4,

$$\Delta(\theta + u) = \Delta^*(\theta) + Ju + \rho(u), \quad \|\rho(u)\| \leq \frac{LJ}{2} \|u\|^2. \quad (71)$$

#### A.5.1. ONE-ROUND COMPARISON: BIAS AND VARIANCE FROM INJECTED NOISE

**Noise-Only Baseline Error** Substituting the linear response into Eq. (70) yields

$$\theta_r^{\text{NO}} = \theta + \eta_{\text{srv}} \Delta^*(\theta) + \underbrace{(I + \eta_{\text{srv}} J)\varepsilon^{(r)}}_{\text{First-Order Injected-Noise Term}} + \eta_{\text{srv}} \rho\left(\varepsilon^{(r)}\right). \quad (72)$$

Thus, even if  $\mathbb{E}[\varepsilon^{(r)}] = 0$ , the state  $\theta_r^{\text{NO}}$  inherits a *first-order* random perturbation  $(I + \eta_{\text{srv}} J)\varepsilon^{(r)}$ .

**MPU Error** In contrast, **MPU** updates the *clean anchor*  $\theta$  using the harmonically denoised estimate  $\bar{\Delta}^{(r)}$ :

$$\theta_r^{\text{MPU}} = \theta + \eta_{\text{srv}} \bar{\Delta}^{(r)} = \theta + \eta_{\text{srv}} \Delta^*(\theta) + \eta_{\text{srv}} \sum_{k=1}^m w_k \rho \left( \epsilon_k^{(r)} \right), \quad (73)$$

where the first-order injected-noise term cancels exactly (Sec. A.2). Consequently, the dominant injected-noise contribution is *second order* in the noise scale (cf. Eq. (38)).

**Variance Comparison** Let  $\Sigma_\epsilon$  denote the covariance of the single-copy baseline noise (e.g., block-diagonal with blocks  $\sigma_\ell^2 I_{d_\ell}$ ). Ignoring the  $O(\|\epsilon\|^2)$  remainder for clarity, Eq. (72) implies

$$\text{Cov}(\theta_r^{\text{NO}} - \theta - \eta_{\text{srv}} \Delta^*(\theta)) \approx (I + \eta_{\text{srv}} J) \Sigma_\epsilon (I + \eta_{\text{srv}} J)^\top, \quad (74)$$

whereas **MPU** exhibits *no* first-order injected-noise covariance term.

#### A.5.2. MULTI-ROUND IMPLICATIONS: NOISE ACCUMULATION VS. DENOISED TRACKING

The contrast becomes more pronounced over multiple rounds. The recursion in Eq. (70) injects fresh noise into the model state at each round, leading—under the linearized view—to a random-walk-like accumulation whose variance grows approximately linearly with  $R$  (modulated by  $I + \eta_{\text{srv}} J$ ). This accumulation can degrade both model utility and unlearning stability.

By contrast, **MPU** never commits the injected noise to the global model state (Algorithm 1). Instead, noise is used solely as a *private publishing perturbation* and its first-order effect is canceled via multi-copy harmonic denoising. As a result, the global iterate tracks the intended unlearning trajectory up to the second-order remainder and reduced client-side randomness.

#### A.5.3. SNR VIEW: TASK-RELEVANT SUBSPACE

If the desired unlearning displacement lies approximately in a low-dimensional task-relevant subspace  $\mathcal{S}$  with projector  $P_{\mathcal{S}}$ , a convenient summary metric is the signal-to-noise ratio (SNR) of the *projected* estimate. Let  $\hat{\Delta}$  be an estimator of  $\Delta^*(\theta)$  and define

$$\text{SNR} = \frac{\|P_{\mathcal{S}} \Delta^*(\theta)\|_F^2}{\text{tr}(P_{\mathcal{S}} \text{Cov}(\hat{\Delta}))}. \quad (75)$$

In the noise-only baseline,  $\text{Cov}(\hat{\Delta})$  contains the first-order term  $J \Sigma_\epsilon J^\top$ , whereas in **MPU** this term is eliminated by design (up to second-order effects). Any independent client-side randomness is further averaged down by  $\sum_k w_k^2 \simeq 1/m$ . This explains why **MPU** more reliably preserves the task-relevant update direction than a single-copy noise-only approach, particularly when  $\text{rank}(\mathcal{S}) \ll d$ .

### A.6. Stability Benefits of Multi-Copy Aggregation

A practical challenge in LLM unlearning is that local optimization can be unstable: the forget set may be small and high-variance, the unlearning objective may be sharp near the current iterate, and common unlearning trainers can produce oscillatory updates when executed from a single initialization. Multi-copy unlearning improves stability by averaging local updates over a small neighborhood around the clean server iterate.

Consider the common case where the local unlearning routine corresponds to (approximately) a gradient step on an unlearning objective  $\mathcal{U}(\theta)$ , so that  $\Delta^*(\theta) \approx -\eta \nabla \mathcal{U}(\theta)$  for some local step size  $\eta$ . Then the aggregated update becomes

$$-\eta \sum_{k=1}^m w_k \nabla \mathcal{U} \left( \theta_{r-1} + \epsilon_k^{(r)} \right) \approx -\eta \mathbb{E}_{\epsilon \sim \mathcal{Q}} [\nabla \mathcal{U}(\theta_{r-1} + \epsilon)], \quad (76)$$

where  $\mathcal{Q}$  is the discrete distribution placing mass  $w_k$  on  $\epsilon_k^{(r)}$ . Equivalently, this is the gradient of a locally averaged objective  $\tilde{\mathcal{U}}(\theta) := \mathbb{E}_{\epsilon \sim \mathcal{Q}} [\mathcal{U}(\theta + \epsilon)]$ . Such local averaging reduces sensitivity to sharp directions near  $\theta_{r-1}$  and makes the effective update direction less erratic, improving stability across rounds.

Importantly, averaging is performed with a *centered, symmetric stencil* of perturbations: our base noises satisfy  $\sum_{k=1}^m \epsilon_{k,\ell}^{0,(r)} \equiv 0$  for every block  $\ell$  (Eq. (2)), and the harmonic weights are chosen to cancel the resulting first-order perturbation in the local linearization (Sec. 3.4). Expanding  $\Delta^*$  around  $\theta_{r-1}$  yields

$$\Delta^* \left( \theta_{r-1} + \epsilon_k^{(r)} \right) = \Delta^* (\theta_{r-1}) + J \epsilon_k^{(r)} + O \left( \left\| \epsilon_k^{(r)} \right\|^2 \right), \quad (77)$$

so harmonic aggregation cancels the  $J \epsilon_k^{(r)}$  term to first order, leaving

$$\bar{\Delta}^{(r)} = \Delta^* (\theta_{r-1}) + O \left( \sum_{k=1}^m w_k \left\| \epsilon_k^{(r)} \right\|^2 \right). \quad (78)$$

Thus, for small perturbation scales, **MPU** tracks the intended (noise-free) unlearning direction while still benefiting from the stabilizing effect of local averaging (the remaining higher-order term acts as a mild, local regularization).

In summary, beyond privacy, the multi-copy mechanism can be viewed as estimating a locally averaged unlearning update around  $\theta_{r-1}$ , which empirically improves stability in settings where single-start unlearning is brittle.

## B. Implementation Details and Supplementary Experiments

This section provides supplementary materials to support a deeper understanding of MPU. It includes detailed descriptions of the benchmarks, evaluation metrics, models, and unlearning algorithms used in our framework, as well as comprehensive implementation details covering the experimental setup, hyperparameters, and prompt templates. We further report additional experimental results and discuss the limitations of MPU.

### B.1. Benchmark

**TOFU** (Task of Fictitious Unlearning), introduced by Maini et al. (2024), is a question–answer (QA) benchmark specifically designed to evaluate the unlearning capabilities of large language models. The dataset comprises QA pairs derived from synthetic autobiographies of 200 fictitious authors, with all content generated by GPT-4 to ensure exclusion from the pretraining corpora of existing LLMs. Each author profile contains 20 QA pairs covering biographical attributes such as name, birthplace, gender, birth year, literary genre, awards, and parental occupations, with book titles seeded from the Goodreads Books dataset to enhance topical diversity.

### B.2. Metrics

For clarity, we categorize the evaluation metrics into three types, summarized below.

#### B.2.1. MEMORIZATION METRICS

These metrics measure the degree to which information from the training data remains encoded in the model after unlearning.

**Probability** We quantify the model’s confidence in generating correct answers by measuring the conditional probability  $P(a | q)$  assigned to the ground-truth answer  $a$  given the question  $q$ , evaluated on **Retain Set**. The resulting score is reported as a normalized probability in  $[0, 1]$ . Following standard practice (Cho et al., 2014), we normalize for answer length by exponentiating the sequence probability by  $1/|a|$ , as formalized in Equation 79:

$$P_{\text{retain}}(x) = P(a | q)^{1/|a|}. \tag{79}$$

For the **Real Authors** and **World Facts** subsets, we evaluate model performance using a relative probability formulation in a multiple-choice setting:

$$P_{\text{real/world}}(x) = \frac{P(a_1 | q)}{\sum_{i=1}^n P(a_i | q)}, \tag{80}$$

where  $q$  denotes a multiple-choice question with candidate answers  $\{a_1, \dots, a_n\}$ , and  $a_1$  corresponds to the ground-truth correct answer. This formulation measures the probability mass assigned to the correct option relative to all candidate choices.

**Recall-Oriented Understudy for Gisting Evaluation (ROUGE)** We adopt ROUGE to quantify the overlap between model-generated answers and the ground-truth responses. In particular, we report ROUGE-L recall (Lin, 2004), which measures similarity via the length of the longest common subsequence (LCS). This metric provides a robust estimate of answer correctness in QA settings by tolerating minor paraphrasing and surface-form variations.

$$\text{ROUGE}_L(x) = \frac{\text{LCS}(a, \hat{a})}{|a|}, \tag{81}$$

where  $\hat{a}$  is the generated answer, and  $\text{LCS}(a, \hat{a})$  is the LCS length between  $a$  and  $\hat{a}$ .

**Truth Ratio** For a given question, we define the *truth ratio*  $R_{\text{Truth}}$  to approximate the relative likelihood assigned by the model to correct versus incorrect answers. Since the model is fine-tuned on a specific canonical phrasing of the ground-truth answer, the corresponding probability may be artificially inflated compared to alternative but semantically equivalent formulations. To mitigate this bias, we evaluate the probability of a paraphrased version of the correct answer rather than the original ground truth.

Likewise, instead of contrasting against a single incorrect response, we consider a set of syntactically similar but factually incorrect answers and compute their average probability. This design yields a more stable and representative estimate of the model’s preference for incorrect information.

Formally, let  $\tilde{a}$  denote a paraphrased correct answer to question  $q$ , and let  $\tilde{x} = [q, \tilde{a}]$ . Let  $A_{\text{err}}$  be a set of incorrect answers  $\{a_{\text{err}}\}$ , constructed by preserving the general textual structure of  $\tilde{a}$  while introducing factual errors. The truth ratio  $R_{\text{Truth}}$  is then defined as:

$$R_{\text{truth}}(x) = \frac{\frac{1}{|A_{\text{err}}|} \sum_{a_{\text{err}} \in A_{\text{err}}} P(a_{\text{err}} | q)^{1/|a_{\text{err}}|}}{P(\tilde{a} | q)^{1/|\tilde{a}|}}. \quad (82)$$

Additionally, as shown in Equation 83, we normalize and rescale the metric to ensure that all values lie within the interval  $[0, 1]$ , with larger values indicating better model performance.

$$R_{\text{adjusted}}(x) = \max(0, 1 - R_{\text{Truth}}(x)). \quad (83)$$

### B.2.2. PRIVACY METRICS

These metrics evaluate whether sensitive information from the forget set can still be inferred or extracted from the model after unlearning. We note that such metrics often rely on idealized assumptions, such as access to perfectly i.i.d. holdout samples or an oracle retain model, which may limit their applicability in practical deployment scenarios.

**Membership Inference Leakage** We could evaluate privacy leakage through membership inference attacks (MIAs), which assess a model’s tendency to memorize training data. Specifically, MIAs test whether an adversary can distinguish between examples drawn from the forget set  $\mathcal{D}_{\text{forget}}$  (members) and unseen examples from a holdout set  $\mathcal{D}_{\text{holdout}}$  (non-members), based on model confidence or loss statistics.

Ideally, a model that has not been trained on  $\mathcal{D}_{\text{forget}}$  should yield an AUC of 0.5, indicating indistinguishability between member and non-member samples. In practice, however, constructing perfectly i.i.d. holdout splits is challenging, and even retrained models may exhibit nontrivial membership signals. Accordingly, following prior benchmarks such as MUSE, we calibrate membership inference results using the AUC score of a retrained reference model, rather than relying on the absolute AUC value alone.

Unlearning generally increases the loss on forgotten samples, but privacy leakage may still arise in two failure modes: (i) **under-unlearning**, where the loss increase is insufficient and membership information remains detectable; and (ii) **over-unlearning**, where the loss becomes abnormally large, again yielding a distinguishable signal. Both cases induce separable loss distributions between  $\mathcal{D}_{\text{forget}}$  and  $\mathcal{D}_{\text{holdout}}$ .

To quantify this effect, we compare the AUC-ROC achieved by the unlearned model  $f_{\text{unlearn}}$  against that of a retrained reference model  $f_{\text{retrain}}$ , and define the relative privacy leakage as

$$\text{PrivLeak} := \frac{\text{AUC}(f_{\text{Unlearn}}; \mathcal{D}_{\text{Forget}}, \mathcal{D}_{\text{Holdout}}) - \text{AUC}(f_{\text{Retrain}}; \mathcal{D}_{\text{Forget}}, \mathcal{D}_{\text{Holdout}})}{\text{AUC}(f_{\text{Retrain}}; \mathcal{D}_{\text{Forget}}, \mathcal{D}_{\text{Holdout}})}. \quad (84)$$

A well-behaved unlearning algorithm should yield a PrivLeak value close to zero, indicating privacy leakage comparable to retraining. In contrast, under-unlearning and over-unlearning result in large negative and positive deviations, respectively, reflecting increased membership distinguishability.

**Forget Quality** In our setting, let  $F_U(x)$  and  $F_R(x)$  denote the empirical cumulative distribution functions (CDFs) of a chosen privacy-related statistic (e.g., Truth Ratio) computed from the unlearned and retained models, based on  $n$  and  $m$  samples, respectively. We employ the Kolmogorov–Smirnov (KS) test to quantify the discrepancy between these two distributions, with the test statistic defined as

$$D_{n,m} = \sup_x |F_U(x) - F_R(x)|. \quad (85)$$

This statistic measures the maximum deviation between the two empirical CDFs, providing a non-parametric assessment of the distributional shift induced by the unlearning procedure.

Under the null hypothesis that the two sample sets are drawn from the same underlying distribution, the hypothesis is rejected at significance level  $\alpha$  if

$$D_{n,m} > c(\alpha) \sqrt{\frac{n+m}{nm}}, \quad (86)$$

where  $c(\alpha)$  is the KS critical value given by

$$c(\alpha) = \sqrt{-\frac{1}{2} \ln \left( \frac{\alpha}{2} \right)}. \quad (87)$$

We define the corresponding  $p$ -value as the smallest significance level  $\alpha$  at which the null hypothesis can be rejected:

$$Q_{\text{forget}} = p = \min \left\{ \alpha \mid D_{n,m} > c(\alpha) \sqrt{\frac{n+m}{nm}} \right\}. \quad (88)$$

Consequently, **Forget Quality** quantifies the statistical confidence with which we can assert that the distributions of Truth Ratio values over the forget set differ between the unlearned and retained models.

### B.2.3. UTILITY METRICS

The objective of unlearning is to effectively remove the influence of targeted data while preserving the model’s performance on non-forget data. Utility metrics evaluate whether the unlearned model maintains its capabilities on tasks beyond the retain set, thereby ensuring that unlearning does not degrade general performance on real-world data distributions.

**Model Utility** Model Utility (MU) measures the retained performance of a model after unlearning, covering both the closely related retain set and broader general-knowledge tasks.

Following the TOFU benchmark protocol, MU is computed as the harmonic mean of nine metrics spanning three data levels: **Retain Set**, **Real Authors**, and **World Facts**. At each level, three metrics are evaluated: **Probability**, **ROUGE**, and **Truth Ratio**, to ensure balanced assessment across memorization, semantic accuracy, and factual correctness.

$$U_{\text{model}} = \frac{9}{\sum_{m \in M} \frac{1}{m}}, \quad (89)$$

where  $M$  denotes the set of all evaluated metrics.

### B.3. Unlearning Algorithms

In this section, we introduce the seven unlearning algorithms instantiated within MPU as modular optimization objectives.

**Notation** Let  $\mathcal{D}_{\text{forget}}$  and  $\mathcal{D}_{\text{retain}}$  denote the forget and retain sets, respectively, and let  $f_\theta$  be the model being updated during unlearning. For an input–output (prompt–completion) pair  $(x, y)$  under a causal LM, we define

$$\log p_\theta(y \mid x) = \sum_{t=1}^{|y|} \log p_\theta(y_t \mid y_{<t}, x), \quad \ell_{\text{CE}}(y \mid x; f_\theta) = -\log p_\theta(y \mid x). \quad (90)$$

Unless otherwise stated, we optionally include a retain regularizer:

$$\mathcal{L}_{\text{retain}}(\theta) = \mathbb{E}_{(x,y) \sim \mathcal{D}_{\text{retain}}} \ell_{\text{CE}}(y \mid x; f_\theta), \quad (91)$$

and optimize  $\min_\theta \mathcal{L}_{\text{forget}}(\theta) + \alpha \mathcal{L}_{\text{retain}}(\theta)$ , where  $\alpha \geq 0$  controls the forgetting–retention trade-off.

#### B.3.1. GRADASCENT (JANG ET AL., 2023)

Gradient Ascent (GradAscent) directly “reverses” standard likelihood training on the forget set by maximizing the cross-entropy (equivalently, minimizing the log-likelihood). Under the minimization convention, the forget objective is

$$\mathcal{L}_{\text{forget}}^{\text{GA}}(\theta) = -\mathbb{E}_{(x,y_f) \sim \mathcal{D}_{\text{forget}}} \ell_{\text{CE}}(y_f \mid x; f_\theta) = \mathbb{E}_{(x,y_f) \sim \mathcal{D}_{\text{forget}}} \log p_\theta(y_f \mid x). \quad (92)$$

This objective is effective at reducing the model likelihood on targeted samples, but without an explicit retention constraint, it may cause collateral degradation on non-forgotten behavior.

### B.3.2. GRADDIFF (LIU ET AL., 2022A)

GradDiff augments GradAscent with a retain loss to explicitly preserve utility on non-forgotten data. A common instantiation writes the full objective as

$$\min_{\theta} \mathcal{L}^{\text{GradDiff}}(\theta) = -\lambda_f \mathbb{E}_{(x, y_f) \sim \mathcal{D}_{\text{forget}}} \ell_{\text{CE}}(y_f | x; f_{\theta}) + \lambda_r \mathbb{E}_{(x, y) \sim \mathcal{D}_{\text{retain}}} \ell_{\text{CE}}(y | x; f_{\theta}), \quad (93)$$

where  $\lambda_f, \lambda_r > 0$  trade off forgetting strength and retention fidelity.

### B.3.3. DPO (RAFAILOV ET AL., 2023)

Direct Preference Optimization (DPO) is a preference-learning objective originally proposed for alignment. Given a preference dataset  $\mathcal{D}_{\text{pref}}$  of triples  $(x, y_w, y_l)$  (preferred  $y_w$  vs. dispreferred  $y_l$ ) and a reference model  $f_{\text{ref}}$ , DPO optimizes

$$\mathcal{L}^{\text{DPO}}(\theta) = -\mathbb{E}_{(x, y_w, y_l) \sim \mathcal{D}_{\text{pref}}} \log \sigma \left( \beta \log \frac{p(y_w | x; f_{\theta})}{p(y_w | x; f_{\text{ref}})} - \beta \log \frac{p(y_l | x; f_{\theta})}{p(y_l | x; f_{\text{ref}})} \right), \quad (94)$$

where  $\beta > 0$  controls the sharpness of preference separation. In unlearning-style instantiations, one can construct preference pairs so that generations containing forget targets are treated as dispreferred.

### B.3.4. NPO (ZHANG ET AL., 2024)

Negative Preference Optimization (NPO) reformulates unlearning as a bounded, alignment-inspired objective that discourages the forget targets relative to a frozen reference model. Let  $f_{\text{ref}}$  denote the reference model (typically the pre-unlearning checkpoint) and  $\sigma(\cdot)$  the sigmoid. The NPO’s forget loss is

$$\mathcal{L}_{\text{forget}}^{\text{NPO}}(\theta) = -\frac{2}{\beta} \mathbb{E}_{(x, y_f) \sim \mathcal{D}_{\text{forget}}} \log \sigma \left( -\beta \log \frac{p(y_f | x; f_{\theta})}{p(y_f | x; f_{\text{ref}})} \right), \quad (95)$$

where  $\beta > 0$  is a temperature parameter. In practice, NPO is often combined with the retain regularizer  $\alpha \mathcal{L}_{\text{retain}}(\theta)$  to preserve utility.

### B.3.5. SIMNPO (FAN ET AL., 2024)

SimNPO removes the explicit reference model and introduces a margin/offset term (denoted  $\gamma$  in the original paper) while retaining the stabilized log-sigmoid form:

$$\mathcal{L}_{\text{forget}}^{\text{SimNPO}}(\theta) = -\frac{2}{\beta} \mathbb{E}_{(x, y_f) \sim \mathcal{D}_{\text{forget}}} \log \sigma \left( -\frac{\beta}{|y_f|} \log p(y_f | x; f_{\theta}) - \gamma \right), \quad (96)$$

where  $|y_f|$  is the target sequence length (used for normalization), and  $\gamma \geq 0$  calibrates the separation threshold. As with other unlearning objectives, SimNPO is commonly paired with  $\alpha \mathcal{L}_{\text{retain}}(\theta)$ .

### B.3.6. UNDIAl (DONG ET AL., 2025)

UnDIAL (Unlearning via Self-Distillation on Adjusted Logits) stabilizes unlearning by defining an explicit, fixed target distribution and distilling the model toward it. Let  $f_{\text{orig}}$  be the frozen pre-unlearning model. For a forget example  $(x, y_f)$  and each position  $t$ , let  $\mathbf{z}_t^{\text{orig}}$  be the teacher logits and  $\mathbf{e}_{y_f, t}$  the one-hot vector of the target token. UnDIAL constructs adjusted logits and a target distribution:

$$\mathbf{z}_t^{\text{adj}} = \mathbf{z}_t^{\text{orig}} - \gamma_{\text{UD}} \mathbf{e}_{y_f, t}, \quad \mathbf{p}_t^{\text{adj}} = \text{softmax}(\mathbf{z}_t^{\text{adj}}), \quad (97)$$

where  $\gamma_{\text{UD}} > 0$  controls the strength of demoting the memorized token. The self-distillation (cross-entropy) unlearning objective is

$$\mathcal{L}_{\text{forget}}^{\text{UnDIAL}}(\theta) = \mathbb{E}_{(x, y_f) \sim \mathcal{D}_{\text{forget}}} \left[ \sum_{t=1}^{|y_f|} \mathcal{H}(\mathbf{p}_t^{\text{adj}}, p(\cdot | x, y_{f, < t}; f_{\theta})) \right], \quad (98)$$

where  $\mathcal{H}(\cdot, \cdot)$  is the cross-entropy between the fixed adjusted distribution and the student model’s predictive distribution. Optionally, UnDIAL can also be combined with  $\alpha \mathcal{L}_{\text{retain}}(\theta)$  for utility preservation.

### B.3.7. SATIMP (YANG ET AL., 2025)

Saturated Importance (SatImp) is a token-wise soft reweighting strategy for enhancing unlearning. It fits into the general token-wise reweighted objective

$$\mathcal{L}_{\text{forget}}(\theta) = \mathbb{E}_{(x, y_f) \sim \mathcal{D}_{\text{forget}}} \sum_{k=1}^{|y_f|} w_{x, y_f, k} \log p(y_{f, k} | y_{f, < k}, x; f_{\theta}). \quad (99)$$

SatImp defines the weight function as

$$w_{x, y_f, k}^{\text{satimp}} = p(y_{f, k} | y_{f, < k}, x; f_{\theta})^{\beta_1} \cdot \left(1 - p(y_{f, k} | y_{f, < k}, x; f_{\theta})\right)^{\beta_2}, \quad (100)$$

where  $\beta_1, \beta_2 \geq 0$  control the smoothness and shape of the weight distribution. As with other objectives, SatImp is commonly paired with  $\alpha \mathcal{L}_{\text{retain}}(\theta)$ .

## B.4. Experimental Settings

### B.4.1. TESTBED

**Hardware Configuration** All experiments are conducted on two Elastic Compute Service (ECS) instances.

For experiments using **Llama-3.2-1B-Instruct** and **Qwen2.5-1.5B-Instruct**, we employ an instance equipped with an Intel Xeon Gold 6462C CPU (16 available cores), 128 GB RAM, 512 GB of available disk space, and an NVIDIA L20 GPU with 48 GB memory. For experiments using **Llama-3.2-3B-Instruct** and **Qwen2.5-3B-Instruct**, we use an instance equipped with an Intel Xeon Platinum 8469C CPU (24 available cores), 128 GB RAM, 512 GB of available disk space, and an NVIDIA HGX H20 GPU with 96 GB memory.

For reproducibility and consistent performance, we recommend the `ecs.gn8is.4xlarge` and `ecs.gn8v.6xlarge` instance types on Alibaba Cloud.

**Software Environment** All experiments are performed on Ubuntu 22.04.5 LTS with NVIDIA driver version 570.195.03 and CUDA 12.8. **MPU** framework is implemented in Python 3.12.12 using PyTorch 2.9.1, and is developed on top of **OpenUnlearning** framework. All unlearning algorithms are instantiated using the implementations integrated within OpenUnlearning. The baseline unlearning models are initialized from the publicly released checkpoints provided by OpenUnlearning on Hugging Face: <https://huggingface.co/open-unlearning>.

Table 4. Default configurations and hyperparameters used in our experiments.

Notation	Hyperparameter	Value	Explanation
<b>General Training Configuration</b>			
–	Random Seed	0	Seed for reproducibility
–	Precision	bfloat16	Numerical precision used for training
–	Attention Backend	FlashAttention-2	Optimized attention implementation
–	Optimizer	paged.adamw_32bit	Memory-efficient AdamW variant
$\lambda_{\text{wd}}$	Weight Decay	0.01	$\ell_2$ regularization coefficient
$B$	Batch Size	32	Number of samples per batch
<b>Server-Side Configuration</b>			
$R$	Global Communication Rounds	See Tab. 9	Total number of server–client rounds
$m$	Copy Number	2	Number of perturbed model copies per round
$\kappa$	Noise Level	0.01	Global multiplier for block-wise noise scales $\{\sigma_{\ell}\}$
$\alpha_k$	Noise Scaling	$1 + \frac{k-1}{m-1}$	Used to match noise magnitude in the single-copy <i>Noised</i> baseline and <b>MPU</b>
$\eta_{\text{srv}}$	Server Step Size	1.0	Step size for applying the aggregated update $\bar{\Delta}^{(r)}$
<b>Client-Side Local Unlearning Configuration</b>			
–	Unlearning Algorithms	See Appx. B.3	Unlearning trainer executed on each published copy
$E_{\text{cli}}$	Local Client Epoch	See Tab. 9	Local unlearning epochs per copy per round
$\eta_{\text{cli}}$	Client Learning Rate	$1 \times 10^{-5}$	Learning rate used by the chosen client unlearning trainer

#### B.4.2. HYPERPARAMETERS

The key hyperparameters used in our experiments across different domains are summarized in Table 4.

We configure the training schedule by selecting the number of global communication rounds (**R**) and local client epochs per round (**E**) based on the client-side unlearning method. Specifically, **GradAscent**, **GradDiff**, and **UnDIAL** use a single-round schedule with  $(R, E) = (1, 10)$ ; **SimNPO**, **DPO**, and **SatImp** use a more communication-intensive schedule with  $(R, E) = (10, 1)$ ; and **NPO** and **WGA** adopt an intermediate configuration with  $(R, E) = (2, 5)$ . For any unspecified method, we default to  $(R, E) = (1, 10)$ .

#### B.4.3. PROMPT TEMPLATE

The chat template is enabled during training. User queries and assistant responses follow the format, as illustrated in Figure 3 and Figure 4.

##### Prompt: Llama-3.2 Series Template

**System Prompt:** You are a helpful assistant.  
**System Prompt with Special Tokens:** <|begin\_of\_text|><|start\_header\_id|>  
system<|end\_header\_id|>\n\nYou are a helpful assistant.<|eot\_id|>  
**User Start Tag:** <|start\_header\_id|>user<|end\_header\_id|>\n\n  
**User End Tag:** <|eot\_id|>  
**Asst Start Tag:** <|start\_header\_id|>assistant<|end\_header\_id|>\n\n  
**Asst End Tag:** <|eot\_id|>  
**Data String:** 10 Apr 2025

Figure 3. Prompt template for Llama-3.2 series.

##### Prompt: Qwen Series Template

**System Prompt:** You are a helpful assistant.  
**System Prompt with Special Tokens:** <|im\_start|>system\nYou are a helpful assistant.<|im\_end|>\n  
**User Start Tag:** <|im\_start|>user\n  
**User End Tag:** <|im\_end|>\n  
**Asst Start Tag:** <|im\_start|>assistant\n  
**Asst End Tag:** <|im\_end|>\n

Figure 4. Prompt template for Qwen2.5 series.

## B.5. Supplementary Experimental Results

Table 5. Performance comparison of different unlearning algorithms using the **Llama-3.2-3B** and **Qwen2.5-3B** models on the TOFU benchmark (Split99). Results are reported under two settings: **Clean**, a noise-free baseline; and **MPU**, using  $m=2$  copies with noise level  $\kappa=0.01$ . Higher values indicate better performance for Forget Quality, Forget Truth Ratio, and Model Utility, while values of PrivLeak closer to 0 are preferred.

Unlearning Algorithms	Forget Quality $\uparrow$			Forget Truth Ratio $\uparrow$			Model Utility $\uparrow$			PrivLeak		
	CLEAN	NOISED	MPU	CLEAN	NOISED	MPU	CLEAN	NOISED	MPU	CLEAN	NOISED	MPU
<b>Llama-3.2-3B-Instruct</b>												
GRADASCENT [ACL 2023]	<b>3.06e-11</b>	5.91e-14	4.47e-16	<b>0.187</b>	0.157	0.142	<b>8.23e-5</b>	7.71e-5	2.28e-5	50.6	53.0	<b>45.9</b>
GRADDIFF [PMLR 2022]	5.41e-2	2.86e-2	<b>5.41e-2</b>	<b>0.504</b>	0.476	0.485	<b>0.419</b>	0.384	0.409	108.0	<b>106.0</b>	107.0
DPO [NEURIPS 2023]	0.579	<b>0.766</b>	0.579	0.685	<b>0.691</b>	0.683	<b>0.634</b>	0.634	0.633	-10.2	-15.3	<b>-3.95</b>
NPO [COLM 2024]	0.990	0.990	<b>0.990</b>	0.635	<b>0.636</b>	0.634	0.650	<b>0.653</b>	0.651	61.2	62.1	<b>57.5</b>
SIMNPO [NEURIPS 2025]	9.71e-2	9.71e-2	<b>9.71e-2</b>	0.550	0.550	<b>0.554</b>	0.658	<b>0.662</b>	0.656	<b>-62.4</b>	-72.3	-64.3
UNDIAL [NAACL 2025]	2.86e-2	<b>5.41e-2</b>	2.86e-2	<b>0.567</b>	0.566	0.563	0.693	0.692	<b>0.693</b>	-72.0	<b>-71.8</b>	-73.3
SATIMP [ICML2025]	1.43e-2	1.43e-2	<b>2.86e-2</b>	0.510	0.507	<b>0.512</b>	0.659	<b>0.661</b>	0.659	<b>-99.7</b>	-100.0	-99.9
<b>Qwen2.5-3B-Instruct</b>												
GRADASCENT [ACL 2023]	0.579	1.86e-23	<b>0.579</b>	0.709	6.4e-20	<b>0.709</b>	<b>0.392</b>	0.000	0.391	-28.7	<b>8.57</b>	-28.1
GRADDIFF [PMLR 2022]	0.766	3.02e-3	<b>0.766</b>	<b>0.712</b>	0.463	0.710	0.394	0.237	<b>0.395</b>	-28.0	67.7	<b>-27.1</b>
DPO [NEURIPS 2023]	0.766	0.919	<b>0.766</b>	0.711	<b>0.733</b>	0.709	0.397	<b>0.412</b>	0.397	-28.9	84.4	<b>-28.8</b>
NPO [COLM 2024]	0.766	0.266	<b>0.766</b>	0.712	<b>0.724</b>	0.711	0.398	<b>0.420</b>	0.397	<b>-28.5</b>	90.5	<b>-28.5</b>
SIMNPO [NEURIPS 2025]	0.766	<b>0.919</b>	0.766	0.712	<b>0.726</b>	0.710	<b>0.398</b>	0.388	0.397	-28.5	<b>-18.9</b>	-28.6
UNDIAL [NAACL 2025]	0.766	<b>0.919</b>	0.766	0.710	<b>0.734</b>	0.711	0.398	<b>0.405</b>	0.396	-28.1	<b>4.17</b>	-28.8
SATIMP [ICML2025]	0.766	0.766	<b>0.766</b>	0.711	<b>0.714</b>	0.712	0.397	0.387	<b>0.397</b>	-28.9	<b>-24.9</b>	-28.7

Table 6. Performance comparison of different unlearning algorithms using the **Llama-3.2-1B** model under **MPU** on the TOFU benchmark (Split99), with varying noise levels  $\kappa \in \{0, 0.05, 0.1\}$  and fixed perturbed copies  $m=2$ . Higher values indicate better performance for Forget Quality, Forget Truth Ratio, and Model Utility, while values of PrivLeak closer to 0 are preferred.

Unlearning Algorithms	Forget Quality $\uparrow$				Forget Truth Ratio $\uparrow$				Model Utility $\uparrow$				PrivLeak			
	$\kappa=0$	$\kappa=0.01$	$\kappa=0.05$	$\kappa=0.1$	$\kappa=0$	$\kappa=0.01$	$\kappa=0.05$	$\kappa=0.1$	$\kappa=0$	$\kappa=0.01$	$\kappa=0.05$	$\kappa=0.1$	$\kappa=0$	$\kappa=0.01$	$\kappa=0.05$	$\kappa=0.1$
GRADASCENT	6.76e-3	5.41e-2	<b>0.579</b>	1.43e-2	0.440	0.468	<b>0.534</b>	0.430	1.39e-4	2.31e-4	<b>3.06e-4</b>	1.49e-4	67.9	69.6	<b>68.0</b>	69.1
GRADDIFF	<b>0.405</b>	0.405	0.266	0.400	0.546	<b>0.547</b>	0.544	0.553	0.468	0.464	<b>0.474</b>	0.472	<b>75.3</b>	77.2	76.5	76.7
DPO	<b>0.266</b>	0.266	0.266	0.165	0.640	<b>0.641</b>	0.641	0.637	0.592	0.591	<b>0.594</b>	0.594	<b>-30.1</b>	-28.9	-29.2	-28.7
NPO	<b>0.919</b>	0.919	0.919	0.919	0.621	0.628	<b>0.624</b>	0.618	0.595	<b>0.597</b>	0.599	0.596	27.7	28.2	<b>26.8</b>	28.1
SIMNPO	5.41e-2	<b>9.71e-2</b>	9.71e-2	5.41e-2	0.520	0.525	<b>0.526</b>	0.525	0.596	<b>0.598</b>	0.598	0.597	<b>-72.4</b>	-71.8	-72.1	-71.7
UNDIAL	<b>1.43e-2</b>	1.43e-2	1.43e-2	1.43e-2	0.528	<b>0.529</b>	0.527	0.526	0.614	<b>0.615</b>	0.615	0.613	<b>-78.3</b>	-78.0	-78.2	-78.0
SATIMP	<b>6.76e-3</b>	6.76e-3	3.02e-3	6.76e-3	0.474	<b>0.476</b>	0.475	0.475	<b>0.601</b>	0.601	0.600	0.600	<b>-99.3</b>	-98.9	-99.2	-99.2

Table 7. Performance comparison of different unlearning algorithms using the **Llama-3.2-1B** model under no-denoise setting on the TOFU benchmark (Split99), with varying noise levels  $\kappa \in \{0, 0.05, 0.1\}$  and fixed perturbed copies  $m=2$ . Additionally, we multiply  $\kappa$  by the expected scaling factor in **MPU** ( $\mathbb{E}_k(\alpha_k) = 1.5$ ). Higher values indicate better performance for Forget Quality, Forget Truth Ratio, and Model Utility, while values of PrivLeak closer to 0 are preferred.

Unlearning Algorithms	Forget Quality $\uparrow$			Forget Truth Ratio $\uparrow$			Model Utility $\uparrow$			PrivLeak		
	$\kappa=0.015$	$\kappa=0.075$	$\kappa=0.15$	$\kappa=0.015$	$\kappa=0.075$	$\kappa=0.15$	$\kappa=0.015$	$\kappa=0.075$	$\kappa=0.15$	$\kappa=0.015$	$\kappa=0.075$	$\kappa=0.15$
GRADASCENT	2.81e-8	1.12e-9	<b>1.23e-7</b>	0.246	0.190	<b>0.252</b>	0.000	0.000	<b>4.11e-5</b>	58.9	<b>57.4</b>	66.4
GRADDIFF	0.266	0.266	<b>0.405</b>	0.533	0.534	0.546	0.461	<b>0.466</b>	0.463	73.3	75.4	<b>72.3</b>
DPO	<b>0.165</b>	0.097	0.165	<b>0.620</b>	0.618	0.620	<b>0.595</b>	0.595	0.595	-19.8	<b>-20.0</b>	-20.0
NPO	<b>0.766</b>	0.766	0.766	<b>0.640</b>	0.623	0.622	<b>0.600</b>	0.599	0.597	<b>32.9</b>	35.4	33.3
SIMNPO	<b>5.41e-2</b>	5.41e-2	5.41e-2	0.522	0.522	<b>0.523</b>	0.592	0.593	<b>0.597</b>	-70.2	-71.8	<b>-72.1</b>
UNDIAL	<b>1.43e-2</b>	1.43e-2	1.43e-2	<b>0.527</b>	0.526	0.527	0.614	0.614	<b>0.616</b>	<b>-77.4</b>	-77.3	-77.2
SATIMP	<b>6.76e-3</b>	6.76e-3	6.76e-3	0.470	<b>0.471</b>	0.471	0.597	0.597	<b>0.598</b>	-99.1	<b>-99.2</b>	-99.2

Table 8. Performance comparison of different unlearning algorithms using the **Llama-3.2-1B** model under **MPU** on the TOFU benchmark (Split99), with varying numbers of perturbed copies  $m \in \{2, 3, 4\}$  and noise level  $\kappa=0.01$ . Higher values indicate better performance for Forget Quality, Forget Truth Ratio, and Model Utility, while values of PrivLeak closer to 0 are preferred.

Unlearning Algorithms	Forget Quality $\uparrow$			Forget Truth Ratio $\uparrow$			Model Utility $\uparrow$			PrivLeak		
	$m=2$	$m=3$	$m=4$	$m=2$	$m=3$	$m=4$	$m=2$	$m=3$	$m=4$	$m=2$	$m=3$	$m=4$
GRADASCENT	5.41e-2	<b>0.165</b>	2.16e-5	0.468	<b>0.500</b>	0.334	<b>2.31e-4</b>	1.68e-4	0.000	69.6	64.0	<b>63.8</b>
GRADDIFF	0.405	0.405	<b>0.579</b>	0.547	0.555	<b>0.570</b>	0.464	<b>0.467</b>	0.467	<b>77.2</b>	77.7	77.4
DPO	0.266	<b>0.579</b>	0.165	<b>0.641</b>	0.631	0.615	0.591	0.592	<b>0.594</b>	-28.9	<b>-22.0</b>	-22.2
NPO	<b>0.919</b>	0.766	0.766	<b>0.628</b>	0.623	0.620	<b>0.597</b>	0.590	0.594	28.2	25.3	<b>25.1</b>
SIMNPO	<b>9.71e-2</b>	5.41e-2	5.41e-2	<b>0.525</b>	0.518	0.519	0.598	0.597	<b>0.599</b>	-71.8	-74.6	<b>-74.1</b>
UNDIAL	<b>1.43e-2</b>	1.43e-2	6.76e-3	<b>0.529</b>	0.528	0.528	<b>0.615</b>	0.613	0.615	<b>-78.0</b>	-78.0	-78.4
SATIMP	6.76e-3	<b>1.43e-2</b>	3.02e-3	<b>0.476</b>	0.473	0.471	<b>0.601</b>	0.598	0.599	-98.9	-99.2	<b>-99.8</b>

Table 9. Performance comparison of different unlearning algorithms using the **Llama-3.2-1B** model under **MPU** on the TOFU benchmark, across varying global communication rounds (**R**) and local client epochs (**E**), with fixed perturbed copies  $m=2$  and noise level  $\kappa=0.01$ . Higher values indicate better performance for Forget Quality and Model Utility, while values of PrivLeak closer to 0 are preferred.

Unlearning method	Forget Quality $\uparrow$				Model Utility $\uparrow$				PrivLeak			
	R1E10	R2E5	R5E2	R10E1	R1E10	R2E5	R5E2	R10E1	R1E10	R2E5	R5E2	R10E1
GRADASCENT	<b>5.41e-2</b>	1.86e-23	1.86e-23	1.86e-23	<b>2.31e-4</b>	0.00	0.000	0.000	69.6	35.2	-2.24	25.6
GRADDIFF	<b>0.405</b>	1.43e-2	5.04e-4	1.95e-10	0.464	0.484	0.494	<b>0.578</b>	77.2	86.8	88.9	88.9
DPO	5.41e-2	0.165	0.165	<b>0.266</b>	0.584	0.591	<b>0.592</b>	0.591	-49.5	-42.1	-17.9	-28.9
NPO	0.766	<b>0.919</b>	<b>0.919</b>	<b>0.919</b>	0.584	<b>0.597</b>	0.592	0.594	51.8	28.2	34.7	40.7
SIMNPO	2.86e-2	2.86e-2	<b>9.71e-2</b>	<b>9.71e-2</b>	0.599	<b>0.601</b>	0.598	0.598	-78.0	-80.5	-75.6	-71.8
UNDIAL	<b>1.43e-2</b>	6.76e-3	<b>1.43e-2</b>	6.76e-3	0.615	<b>0.617</b>	0.612	0.615	-78.0	-82.8	-77.6	-84.2
SATIMP	<b>6.76e-3</b>	3.02e-3	<b>6.76e-3</b>	<b>6.76e-3</b>	0.600	0.599	0.598	<b>0.601</b>	-99.9	-99.8	-99.3	-98.9

Table 10. Performance comparison of different unlearning algorithms using the **Llama-3.2-1B** model under **MPU** on the TOFU benchmark, across varying split strategies (FORGET01, FORGET05, and FORGET10), with fixed perturbed copies  $m=2$  and noise level  $\kappa=0.01$ . Higher values indicate better performance for Forget Quality, Forget Truth Ratio, and Model Utility, while values of PrivLeak closer to 0 are preferred.

Unlearning Algorithms	Forget Quality $\uparrow$			Forget Truth Ratio $\uparrow$			Model Utility $\uparrow$			PrivLeak		
	FORGET01	FORGET05	FORGET10	FORGET01	FORGET05	FORGET10	FORGET01	FORGET05	FORGET10	FORGET01	FORGET05	FORGET10
GRADASCENT	<b>5.41e-2</b>	1.94e-119	1.06e-239	<b>0.468</b>	1.71e-23	1.74e-22	<b>2.31e-4</b>	0.000	0.000	69.6	-28.0	<b>-21.6</b>
GRADDIFF	<b>0.405</b>	5.99e-105	8.51e-237	<b>0.547</b>	0.002	3.09e-10	<b>0.464</b>	0.421	0.264	77.2	<b>56.8</b>	61.8
DPO	<b>0.266</b>	4.30e-3	9.07e-8	<b>0.641</b>	0.574	0.545	0.591	0.595	<b>0.598</b>	-28.9	-43.7	<b>-59.0</b>
NPO	<b>0.919</b>	0.112	4.46e-6	<b>0.628</b>	0.603	0.555	0.597	0.614	<b>0.623</b>	28.2	<b>-4.00</b>	-0.946
SIMNPO	<b>9.71e-2</b>	4.61e-7	5.42e-13	<b>0.525</b>	0.514	0.498	<b>0.598</b>	0.595	0.598	-71.8	-77.7	<b>-82.0</b>
UNDIAL	<b>1.43e-2</b>	2.44e-10	7.98e-17	0.529	0.521	<b>0.531</b>	0.615	0.615	<b>0.616</b>	-78.0	-91.7	<b>-94.9</b>
SATIMP	<b>6.76e-3</b>	1.33e-13	2.81e-20	<b>0.476</b>	0.471	0.469	<b>0.601</b>	0.593	0.597	-98.9	<b>-99.9</b>	-99.2

Table 11. Baseline performance of the OpenUnlearning Framework without MPU, using the Llama-3.2-1B and Llama-3.2-3B models under MPU on the TOFU benchmark (Split99). Higher values indicate better performance for Forget Quality, Forget Truth Ratio, and Model Utility, while values of PrivLeak closer to 0 are preferred.

Unlearning Algorithms	Forget Quality $\uparrow$			Forget Truth Ratio $\uparrow$			Model Utility $\uparrow$			PrivLeak		
	FORGET01	FORGET05	FORGET10	FORGET01	FORGET05	FORGET10	FORGET01	FORGET05	FORGET10	FORGET01	FORGET05	FORGET10
<b>Llama-3.2-1B-Instruct</b>												
GRADASCENT	<b>6.58e-5</b>	1.94e-119	1.06e-239	<b>0.355</b>	2.12e-23	1.27e-22	0.000	0.000	0.000	65.8	<b>-28.4</b>	-21.1
GRADDIFF	<b>0.405</b>	5.99e-105	8.51e-237	<b>0.535</b>	0.004	7.22e-10	<b>0.461</b>	0.393	0.247	77.1	<b>56.8</b>	61.3
DPO	<b>0.165</b>	2.08e-3	3.08e-7	<b>0.637</b>	0.573	0.545	0.591	0.594	<b>0.598</b>	-25.5	-44.5	<b>-57.8</b>
NPO	<b>0.919</b>	0.112	4.58e-7	<b>0.624</b>	0.595	0.551	0.599	0.614	<b>0.619</b>	30.6	<b>-2.11</b>	3.78
SIMNPO	<b>5.41e-2</b>	1.46e-7	2.73e-12	<b>0.526</b>	0.510	0.498	<b>0.598</b>	0.593	0.597	-68.4	-76.6	<b>-82.4</b>
UNDIAL	<b>1.43e-2</b>	4.87e-10	4.24e-17	0.530	0.524	<b>0.531</b>	0.613	0.615	<b>0.618</b>	-76.4	-91.6	<b>-94.8</b>
SATIMP	<b>3.02e-3</b>	2.96e-13	1.12e-19	<b>0.474</b>	0.471	0.469	<b>0.600</b>	0.594	0.600	-98.9	<b>-99.9</b>	-99.2
<b>Llama-3.2-3B-Instruct</b>												
GRADASCENT	<b>3.06e-11</b>	1.94e-119	1.06e-239	<b>0.187</b>	6.63e-8	4.79e-20	<b>8.23e-5</b>	<b>0.000</b>	0.000	50.6	<b>-22.5</b>	-19.2
GRADDIFF	<b>5.41e-2</b>	1.94e-119	8.51e-237	<b>0.504</b>	2.01e-9	1.20e-10	0.419	<b>0.593</b>	0.345	108	<b>56.3</b>	64.6
DPO	<b>0.579</b>	1.18e-2	2.13e-6	<b>0.685</b>	0.588	0.594	0.634	<b>0.635</b>	0.634	-10.2	-62.0	<b>-69.1</b>
NPO	<b>0.990</b>	0.793	2.99e-2	<b>0.635</b>	0.617	0.581	0.650	<b>0.675</b>	0.673	61.2	9.83	<b>-24.0</b>
SIMNPO	<b>9.71e-2</b>	3.60e-9	1.03e-14	<b>0.550</b>	0.499	0.501	0.658	0.652	<b>0.659</b>	-62.4	-81.0	<b>-86.3</b>
UNDIAL	<b>2.86e-2</b>	3.08e-12	8.08e-22	<b>0.567</b>	0.507	0.515	0.693	<b>0.701</b>	0.696	-72.0	<b>-92.1</b>	-94.3
SATIMP	<b>1.43e-2</b>	2.96e-13	2.05e-24	<b>0.510</b>	0.463	0.469	<b>0.659</b>	0.649	<b>0.659</b>	-99.7	<b>-100</b>	-99.5

## B.6. Supplementary Experimental Analysis

### B.6.1. EFFECT OF COPY NUMBER $m$

We study the sensitivity of MPU to the number of published perturbed copies by varying  $m \in \{2, 3, 4\}$  while keeping the noise level and all other hyperparameters identical to Table 1. Overall, increasing  $m$  can improve stability for high-variance or unstable unlearning routines, but the gains are not necessarily monotonic and may saturate (or regress) for certain algorithms.

For relatively stable algorithms (e.g., UnDIAL and SatImp), metrics are largely invariant to  $m$ . Specifically, UnDIAL maintains FQ  $\approx 0.014$ , and MU  $\approx 0.615$  for  $m=2$  and  $m=3$ , with only a minor FQ drop at  $m=4$ . Similarly, SatImp remains within a narrow band for FTR/MU and exhibits only small FQ variation. This suggests that when the underlying unlearning update is already stable, multi-copy aggregation mainly provides robustness rather than large performance shifts.

For more hyperparameter-sensitive unlearning algorithms, moderate increases in  $m$  can substantially improve forgetting. For example, GradAscent improves from FQ 0.054 at  $m=2$  to 0.165 at  $m=3$ , alongside a higher FTR (0.468  $\rightarrow$  0.500). Likewise, DPO achieves its best FQ at  $m=3$  (FQ 0.579 versus 0.266 at  $m=2$ ), and GradDiff benefits from a larger copy number, reaching FQ 0.579 at  $m=4$ . However, these gains are not uniformly monotonic: GradAscent collapses at  $m=4$  (FQ  $\approx 2.16 \times 10^{-5}$ ), and DPO also drops at  $m=4$ . These patterns indicate that while multi-copy aggregation can stabilize updates, overly aggressive averaging can interact unfavorably with certain training dynamics.

Finally, privacy leakage is generally comparable across  $m$ , with modest improvements for some methods. For instance, NPO reduces  $|\text{PrivLeak}|$  from 28.2 at  $m=2$  to 25.3 and 25.1 at  $m=3$  and  $m=4$ . Taken together,  $m=2$  provides a strong and efficient default, while  $m=3$  can be a favorable choice for stabilizing unstable unlearning algorithms (e.g., GradDiff) without materially sacrificing utility.

### B.6.2. EFFECT OF NOISE LEVEL $\kappa$

We next vary the noise level  $\kappa \in \{0, 0.01, 0.05, 0.1\}$  while keeping all other settings fixed (Table 6). Across most algorithms, MPU is robust to a broad range of  $\kappa$ , with FTR and MU remaining largely stable and only modest variations in privacy leakage.

For strong and stable unlearning methods, performance is nearly invariant to  $\kappa$ . Most notably, NPO maintains identical Forget Quality (FQ = 0.920) across all tested noise levels, while FTR and MU remain in a narrow range. Similarly, UnDIAL keeps FQ = 0.014 and FTR  $\approx 0.53$  across all  $\kappa$ , and SatImp shows only a small dip in FQ at  $\kappa=0.05$ .

For instability-prone methods, moderate noise can act as a stabilizer. GradAscent exhibits a clear non-monotonic trend: FQ increases from 0.007 at  $\kappa=0$  to 0.054 at  $\kappa=0.01$ , peaks at 0.580 for  $\kappa=0.05$ , and then drops again at  $\kappa=0.1$ . This suggests that intermediate noise can regularize unstable unlearning dynamics, whereas overly large noise begins to erode the usefulness of the client update. A similar (but weaker) effect appears for SimNPO, where small-to-moderate noise improves FQ from 0.054 to 0.097.

Overall, these results indicate that MPU tolerates noise injection well, and that small-to-moderate  $\kappa$  can improve stability for certain algorithms without harming model utility. In our default setting,  $\kappa=0.01$  provides a balanced operating point that performs competitively across methods.

### B.6.3. ROUND-EPOCH ALLOCATION UNDER FIXED TOTAL LOCAL COMPUTE

Table 9 studies how the training schedule affects unlearning when the total number of local epochs is fixed to 10 (consistent with the default setting in OpenUnlearning), but allocated differently across global rounds  $R$  and local epochs per round  $E$ . Overall, we observe a round-epoch trade-off: increasing the number of rounds (hence smaller  $E$ ) often improves MU but can weaken FQ, while concentrating training into fewer rounds with larger  $E$  can strengthen forgetting for some algorithms but may risk over-updating in others.

Different unlearning algorithms exhibit distinct sensitivity to the schedule. GradAscent performs best with R1E10, while increasing the number of rounds causes both FQ and MU to collapse to nearly zero, indicating severe instability under repeated round-wise aggregation. In contrast, NPO benefits from R2E5, achieving substantially higher FQ than R1E10 while also improving MU. Similarly, SimNPO prefers more rounds for stronger forgetting, whereas DPO improves forgetting monotonically as the number of rounds increases.

#### B.6.4. NO-DENOISING ABLATION UNDER MATCHED EFFECTIVE NOISE

To isolate the importance of MPU’s denoising aggregation, we evaluate a no-denoise baseline in which the client trains on a single noisy model and no inverse reparameterization or aggregation is applied (Table 7). To ensure a fair comparison, we scale the baseline noise such that the effective noise magnitude matches MPU by multiplying  $\kappa$  by  $\mathbb{E}_\kappa(\alpha_k)=1.5$ .

No-denoise training is markedly less reliable for unstable unlearning algorithms. In particular, GradAscent essentially fails under no-denoise: its FQ remains extremely close to zero (on the order of  $10^{-9}$  to  $10^{-7}$ ), and MU is approximately zero across all tested noise levels. This contrasts sharply with MPU (Table 6), where GradAscent can achieve strong forgetting with FQ 0.579 at  $\kappa=0.05$ .

For moderately stable methods, the no-denoise baseline often requires substantially larger noise to approach comparable forgetting. For example, GradDiff reaches its best FQ (0.405) only at the largest tested noise ( $\kappa=0.15$ ), whereas MPU attains comparable FQ at much smaller noise (e.g.,  $\kappa=0.01$  or even  $\kappa=0$ ). By contrast, for already-stable methods such as NPO and UnDIAL, no-denoise does not provide consistent improvements and often matches (but does not surpass) MPU.

Overall, this ablation supports that multi-copy denoising and harmonic aggregation are key contributors to MPU’s stability—especially for high-variance unlearning updates—enabling strong forgetting at lower noise without sacrificing utility.

#### B.6.5. ROBUSTNESS TO FORGET-SPLIT STRATEGIES

We evaluate MPU under different forget ratios by increasing the amount of data to be forgotten from 1% (FORGET01) to 5% (FORGET05) and 10% (FORGET10), while fixing  $\kappa=0.01$  and  $m=2$  (Table 10). A consistent trend emerges: larger forget splits substantially degrade Forget Quality across nearly all algorithms, indicating that unlearning becomes significantly more challenging as the forget request scales up.

Many methods exhibit dramatic FQ collapse when moving from FORGET01 to FORGET05/10. For instance, GradDiff drops from FQ 0.405 at FORGET01 to effectively zero (e.g.,  $5.99 \times 10^{-105}$  and  $8.51 \times 10^{-237}$ ) at FORGET05 and FORGET10. Even the strongest unlearning algorithm in our comparison, NPO, decreases from FQ 0.919 at FORGET01 to 0.112 at FORGET05 and  $4.46 \times 10^{-6}$  at FORGET10. This suggests that scaling to larger forget partitions likely requires additional tuning (e.g., more rounds, different learning rates, or algorithm-specific regularization) beyond the default hyperparameters tuned for the FORGET01 setting.

Interestingly, model utility is comparatively more robust for several algorithms. SimNPO, DPO, and UnDIAL maintain MU around 0.59–0.62 across all splits, even when FQ collapses. Privacy leakage exhibits mixed behavior: NPO reduces  $|\text{PrivLeak}|$  strongly as the forget split increases (from 28.2 to  $-4.0$  to  $-0.946$ ), whereas DPO and UnDIAL show increased leakage in magnitude (e.g.,  $-28.9 \rightarrow -43.7 \rightarrow -59.0$  and  $-78.0 \rightarrow -91.7 \rightarrow -94.9$ ). These results highlight that scaling the forget ratio can introduce new privacy–forgetting trade-offs that vary across algorithms.

#### B.6.6. SCALING MPU ACROSS MODEL SIZES

Finally, we test whether MPU scales to larger base models by comparing results on **Llama-3.2-1B-Instruct** and **Llama-3.2-3B-Instruct** under multiple forget ratios (Table 11). Overall, MPU remains effective at larger scale, and larger models often provide improved headroom for strong unlearning algorithms—especially under more challenging forget ratios.

Under FORGET01, the 3B model generally attains equal or better forgetting quality and higher utility for several algorithms. For example, NPO improves from FQ 0.919 (1B) to 0.990 (3B) while increasing MU from roughly 0.599 to 0.650. Similarly, preference-based unlearning (DPO) improves substantially with scale, rising FQ from 0.165 (1B) to 0.579 (3B) and MU from 0.591 to 0.634. These patterns suggest that higher-capacity models can better accommodate targeted forgetting updates while preserving general capabilities.

The benefit of scale is even clearer for larger forget splits. For NPO, the 3B model retains strong FQ at FORGET05 (FQ 0.793), whereas the 1B model drops to FQ 0.112. At FORGET10, the 3B model still achieves non-trivial forgetting (FQ 0.030), while the 1B model collapses toward zero. In contrast, some algorithms remain fragile regardless of scale: GradAscent yields near-zero FQ even at FORGET01 for both 1B and 3B, and GradDiff degrades sharply for FORGET05/10 on both models.

For privacy leakage, the sign of PrivLeak can vary, and thus the magnitude (distance to zero) is the relevant indicator. In many cases (e.g., NPO), the magnitude decreases as the forget ratio increases, whereas other methods exhibit large-magnitude

values that worsen under harder forget splits. Overall, Table 11 indicates that **MPU** scales favorably with model size for the most effective unlearning algorithms, and that larger models can better sustain non-trivial forgetting under more demanding forget requests.